# SYNTHESIS OF PHOTOPOLYMERIZABLE MACROMERS GIVING NOVEL POLY(β-AMINO ESTER)S FOR BIOMEDICAL APPLICATIONS

by

Ece Akyol

B.S., Chemistry, Boğaziçi University, 2014

Submitted to the Institute for Graduate Studies in
Science and Engineering in partial fulfillment of
The requirements for the degree of
Master of Science

Graduate Program in Chemistry
Boğaziçi University

2016

# SYNTHESIS OF PHOTOPOLYMERIZABLE MACROMERS GIVING NOVEL POLY(β-AMINO ESTER)S FOR BIOMEDICAL APPLICATIONS

APPROVED BY:

Prof. Duygu Avcı Semiz .....

(Thesis Supervisor)

Assoc. Prof. Havva Funda Yağcı Acar .....

Prof. İlknur Doğan .....

DATE OF APPROVAL: 01.08.2016

*Dedicated to my nieces and nephew...*

# ACKNOWLEDGEMENTS

I would like to deeply thank my supervisor Prof. Duygu Avcı Semiz for her valuable guidance, advices, attention and encouragement throughout my project. I gained a lot of experience thanks to her and I am very appreciated to do master's degree under her supervision.

I want to express my thanks to my committee members Prof. İlknur Doğan and Assoc. Prof. Havva Funda Yağcı Acar for politely sparing their valuable time for reviewing the final manuscript and for their constructive interpretations and recommendations.

I wish to extend my great thanks to Fatma Demir Duman due to her help. I would also like to thank my dear friends İsmail Altınbaşak and Ayşegül Sezer for their friendship and advices. I also thank to my dear group friends Melek Naz Güven, Betül Bingöl, Miraç Tatlıyüz, Tuğçe Nur Eren, Sesil Çınar, Seçkin Altuncu and Türkan Gençoğlu for their friendship.

I would also like to thank all members of Chemistry Department for their helps.

I want to express my gratitude to my mother, father, sisters, brothers and niece for their endless love, support and encouragement throughout my entire life.

Finally, I also want to thank to The Scientific and Technological Research Council of Turkey (TÜBİTAK) [114Z926] for the financial support for my research.

# ABSTRACT

## SYNTHESIS OF PHOTOPOLYMERIZABLE MACROMERS GIVING NOVEL POLY(β-AMINO ESTER)S FOR BIOMEDICAL APPLICATIONS

Biodegradability, hemocompatibility, protein adsorption resistance, and strong interactions with hydroxyapatite (HAP)-based tissues such as dentin, enamel, and bone are properties that make phosphorus-containing biomaterials relevant and important. Here, novel phosphonate-functionalized poly(β-amino ester) (PBAE) macromers are synthesized through aza-Michael addition of various diacrylates [1,6-hexane diol diacrylate (HDDA), poly(ethylene glycol) diacrylate (PEGDA, $M_n$=575), 1,4-butane diol diacrylate (BDDA), 1,6-hexanediol ethoxylatediacrylate (HDEDA), triethyleneglycoldiacrylate (TEGDA)] and two phosphonate-containing primary amines [diethyl 2-aminoethylphosphonate (A1) and diethyl (6-amino hexyl) phosphonate (A2)] efficiently without any catalyst. Macromers prepared from Michael addition of the same acrylates with propyl amine (PA) were used as references. The molecular weights of the macromers were ca. 2000-3000, confirmed by both gel permeation chromatography and $^1$H-NMR spectroscopy. The macromers were used for free radical photopolymerization in the presence of 2,2-dimethoxy-2-phenylacetophenone as photoinitiator and under UV light to give biodegradable gels and the gels' properties (degradation and cell interactions) were studied. The mass loss and cell interactions of the polymers were found to be affected by the chemical structure of the polymers. Polymers based on HDDA, BDDA and HDEDA showed similar and very low mass losses (3-15 % after two weeks) due to their hydrophobic backbone structures. The highest mass losses were observed for PEGDA-based macromers (40-50 % after two weeks). Some of the phosphonate-functionalized PBAE polymers were found to support attachment of SaOS-2 cells better than nonphosphonated ones.

# ÖZET

## BİYOMEDİKAL UYGULAMALAR İÇİN YENİ POLİ(BETA-AMİNO ESTER)LER VEREN FOTOPOLİMERLEŞTİRİLEBİLİR MAKROMERLERİN SENTEZİ

Biyobozunum, kanla uyumluluk, protein adsorbsiyon direnci ve dentin, diş minesi ve kemik gibi HAP-tabanlı dokularla güçlü etkileşim fosfor ihtiva eden biyomalzemeleri önemli yapan özellikleridir. Bu çalışmada,fosfonat grubu içeren yeni poli-β amino ester (PBAE) makromerleri çeşitli diakrilat [1,6-hekzan diol diakrilat (HDDA), poli(etilenglikol) diakrilat (PEGDA, $M_n$=575), 1,4-bütan diol diakrilat (BDDA), 1,6-hekzandiol ethoksilatdiakrilat (HDEDA), trietilenglikoldiakrilat (TEGDA)] ve iki fosfonat içeren birinci derece aminin [dietil 2-aminoetilfosfonat (A1) ve dietil (6-amino hekzil) fosfonat (A2)] Michael katılma reaksiyonu ile katalistsiz sentezlendi. Aynı akrilatların propil aminle Michael katılma reaksiyonuyla elde edilen makromerler referans olarak kullanıldı. Makromerlerin mol ağırlıklarının 2000-3000 civarı olduğu hem jel geçirgenlik kromatografisi hem de $^1$H-NMR spektroskopisiyle doğrulandı. Makromerler 2,2-dimetoksi-2-fenilasetofenon fotobaşlatıcı ve UV ışığı altında serbest radikal fotopolimerizasyonuyla biyobozunur jeller elde etmek için kullanıldı ve bu jellerin özellikleri (bozunuma ve hücre etkileşim) incelendi. Polimerlerin kütle kaybının ve hücre etkileşimlerinin polimerlerin kimyasal yapıları ile ilişkili olduğu bulundu. HDDA, BDDA ve HDEDA temelli polimerler hidrofobik ana zincirlerinden dolayı benzer ve çok düşük kütle kayıpları (iki hafta sonunda 3-15%) gösterdi. En yüksek kütle kayıpları (iki hafta sonunda 40-50%) PEGDA temelli polimerler için bulundu. Fosfonat fonksiyonlu PBAE polimerlerin bazılarının SaOS-2 hücre tutunmasını fosfonat içermeyenlere göre daha fazla desteklediği bulundu.

# TABLE OF CONTENTS

ACKNOWLEDGEMENTS ..... iv

ABSTRACT ..... v

ÖZET ..... vi

LIST OF FIGURES ..... ix

LIST OF TABLES ..... xii

LIST OF SYMBOLS ..... xiv

LIST OF ACRONYMS/ABBREVIATIONS ..... xvii

1. INTRODUCTION ..... 1

1.1. Poly(β-amino ester)s ..... 1

1.1.1 Gene Delivery Applications ..... 1

1.1.2 Drug Delivery Applications ..... 4

1.1.3 Tissue Engineering Applications ..... 8

1.2. Phosphorous Based Biomaterials ..... 13

2. OBJECTIVES ..... 16

3. EXPERIMENTAL WORK ..... 17

3.1. Materials and Characterization ..... 17

3.1.1 Materials ..... 17

3.1.2 Characterization ..... 18

3.2. Synthesis of Starting Materials ..... 18

3.2.1 Synthesis of diethyl 2-aminoethylphosphonate (A1) ..... 18

3.2.2 Synthesis of diethyl (6-amino hexyl) phosphonate (A2) ..... 18

3.3. Synthesis of poly(β-amino ester) macromers ..... 20

3.4. Synthesis of branched poly(β-amino ester) macromers ..... 22

3.5. Synthesis of network polymers ..... 23

3.6. Photopolymerization ..... 23
3.7. Degradation ..... 24
3.8. In Vitro Cytotoxicity Assay ..... 24
3.9. In Vitro Cell Interaction Studies ..... 25
3.10. Statistical Analysis ..... 25
4. RESULTS AND DISCUSSION ..... 26
4.1. Synthesis of amines ..... 26
4.2. Synthesis of PBAE macromers ..... 30
4.3. Synthesis of PBAE network polymers ..... 40
4.4. Photopolymerization studies ..... 40
4.5. Degradation Studies ..... 41
4.6. In vitro cell interaction ..... 43
4.7. In vitro cytotoxicity of polymers ..... 51
5. CONCLUSIONS ..... 53
REFERENCES ..... 54

# LIST OF FIGURES

Figure 1.1. Synthesis of poly(β-amino ester)s. ..... 1

Figure 1.2. Synthesis of end-modified PBAEs [1]. ..... 3

Figure 1.3. PEI terminated PBAE [3]. ..... 4

Figure 1.4. Preparation of PBAEs, PEG-PBAE block copolymers and titration curves of some of PBAEs [9]. ..... 5

Figure 1.5. Structure of MPEG-PBAE block copolymer and dissociation of DOX-loaded micelles under physiological pH [11]. ..... 6

Figure 1.6. Dual redox- and pH-sensitive copolymeric micelles which are prepared for intracellular doxorubicin delivery [15]. ..... 7

Figure 1.7. Synthesis of trigger-responsive PBAE crosslinkers [16]. ..... 7

Figure 1.8. General synthesis scheme and the acrylates and amines used to produce a library of 120 photopolymerizable macromers [17]. ..... 9

Figure 1.9. Degradation behavior of polymers synthesized from one amine and four acrylates [17]. ..... 10

Figure 1.10. Effect of macromer molecular weight on tensile modulus [18]. ..... 11

Figure 1.11. PBAEs synthesized from diacrylates and tetrafunctional primary amines [22]. ..... 12

Figure 1.12. Polymer obtained from the synthesis of diacrylate and multifunctional amine [24]. ..... 12

Figure 1.13. Degradation properties of the hydrogels [24]. ..... 13

Figure 1.14. Self-etching dental adhesive monomers containing phosphoric acids [26]. ... 14

Figure 1.15. Bone targeting systems for carrying bioactive molecules [31]. ..... 14

Figure 1.16. Binding energies of different materials [34]. ..... 15

Figure 1.17. Hydrogels prepared from phosphoester-containing poly(ethyleneglycol) for bone cartilage and tissue engineering [35]. ..... 15

Figure 4.1. Structures of amines. ..... 26

Figure 4.2. Synthesis of A1 [38]. ..... 26

Figure 4.3. $^{1}$H-NMR spectrum of A1. ..... 27

Figure 4.4. Synthesis of A2 [39,40]. ..... 28

Figure 4.5. $^{1}$H-NMR spectrum of N-(6-bromohexyl) phtalimide. ..... 29

Figure 4.6. $^{1}$H-NMR spectrum of diethyl 6-phthalimidohexylphosphonate. ..... 29

Figure 4.7. $^{1}$H-NMR spectrum of diethyl (6-amino hexyl) phosphonate. ..... 30

Figure 4.8. Schematic of macromer synthesis, and structures of acrylates and amines ..... 32

Figure 4.9. $^{1}$H-NMR spectra of HDDA, A1 and HDDA-A1 macromer. ..... 34

Figure 4.10. $^{1}$H-NMR spectra of HDDA-A1 macromers (diacrylate to amine ratio is 1.1:1 and 1.2:1). ..... 35

Figure 4.11. $^{1}$H-NMR spectrum of HDDA-PA macromer (diacrylate to amine ratio is 1.2:1).....35

Figure 4.12. $^{1}$H-NMR spectrum of BDDA-A1 macromer (diacrylate to amine ratio is 1.2:1).....36

Figure 4.13. $^{1}$H-NMR spectrum of HDEDA-A1 macromer (diacrylate to amine ratio is 1.2:1).....36

Figure 4.14. $^{1}$H-NMR spectrum of PEGDA-A1 macromer (diacrylate to amine ratio is 1.2:1).....37

Figure 4.15. $^{1}$H-NMR spectrum of TEGDA-A1 macromer (diacrylate to amine ratio is 1.2:1).....37

Figure 4.16. $^{1}$H-NMR spectrum of PEGDA-PA macromer (diacrylate to amine ratio is 1.2:1).....38

Figure 4.17. $^{1}$H-NMR spectrum of PEGDA-A2 macromer (diacrylate to amine ratio is 1.2:1).....38

Figure 4.18. $^{1}$H-NMR spectrum of HDDA-A2 macromer (diacrylate to amine ratio is 1.2:1). ..... 39

Figure 4.19. FTIR spectra of PEGDA-A1 and HDDA-A1 macromers. ..... 39

Figure 4.20. Gelation bar of all macromers. ..... 40

Figure 4.21. Conversion-time plots of some of the macromers. ..... 41

Figure 4.22. Degradation behavior of various polymers. ..... 42

Figure 4.23. Degradation behavior of various polymers after 2, 4 and 8 weeks ..... 43

Figure 4.24. Photomicrographs of SaOS-2 cells 24 h after seeding on (a) TCPS (control, treated polystyrene tissue culture plates), (b) PS (control, untreated polystyrene plates). ..... 46

Figure 4.25. Photomicrographs of SaOS-2 cells 24 h after seeding on HDDA-PA polymer. ..... 47

Figure 4.26. Photomicrographs of SaOS-2 cells 24 h after seeding on HDDA-A1 polymer. ..... 47

Figure 4.27. Photomicrographs of SaOS-2 cells 24 h after seeding on BDDA-PA polymer. ..... 48

Figure 4.28. Photomicrographs of SaOS-2 cells 24 h after seeding on BDDA-A1 polymer. ..... 48

Figure 4.29. Photomicrographs of SaOS-2 cells 24 h after seeding on HDEDA-PA polymer. ..... 49

Figure 4.30. Photomicrographs of SaOS-2 cells 24 h after seeding on HDEDA-A1 polymer. ..... 49

Figure 4.31. Photomicrographs of SaOS-2 cells 24 h after seeding on PEGDA-PA polymer. ..... 50

Figure 4.32. Photomicrographs of SaOS-2 cells 24 h after seeding on PEGDA-A1 polymer. ..... 50

Figure 4.33. Number of attached cells/area for various polymers under different conditions. ..... 51

Figure 4.34. Viability of SaOS-2 cells in the presence of degredation products after 24 hours incubation as determined by MTT assay ($p < 0.05$(*), $p < 0.01$ (**), $p < 0.001$ (***) and $p < 0.0001$(****)), (n=4). .....51

# LIST OF TABLES

Table 4.1. Solubilities of macromers. ..... 33

Table 4.2. Repeating units (n) of macromers. ..... 33

Table 4.3. GPC results of some of the macromers. ..... 34

# LIST OF SYMBOLS

| | |
|---|---|
| $A_{control}$ | Absorption of control cells |
| $A_{sample}$ | Absorption of treated cells |
| Abs | Absorbance |
| DC | Double bond conversion |
| $M_n$ | Number average molecular weight |
| PDI | Polydispersity index |
| $\lambda_{em}$ | Wavelength of emission |
| $\lambda_{exc}$ | Wavelength of excitation |

# LIST OF ACRONYMS/ABBREVIATIONS

| | |
|---|---|
| A1 | Diethyl 2-aminoethylphosphonate |
| A2 | Diethyl (6-amino hexyl) phosphonate |
| BDDA | 1,4-Butane diol diacrylate |
| DAPI | 4′,6-Diamidino-2-phenylindole |
| DMPA | 2,2-Dimethoxy-2-phenylacetophenone |
| DNA | Deoxyribonucleic acid |
| FITC | Fluorescein isothiocyanate |
| FT-IR | Fourier Transform Infrared Spectroscopy |
| GPC | Gel Permeation Chromatography |
| HDDA | 1,6-Hexane diol diacrylate |
| HDEDA | 1,6-Dexanediol ethoxylatediacrylate |
| MDR | Multiple drug resistance |
| MTT | Thiazolyl blue tetrazolium bromide |
| NMR | Nuclear Magnetic Resonance spectroscopy |
| PA | Propyl amine |
| PBAE | Poly β-amino ester |
| PBS | Phosphate buffered saline |
| PEGDA | Poly(ethylene glycol) diacrylate |
| PEI | Polyethylene imine |
| RGDC | cyclo(Arg-Gly-Asp-D-Phe-Cys) peptide |
| RNA | Ribonucleic acid |
| SaOS-2 | Human osteogenic sarcoma cells |
| TMPTA | Trimethyloyl propane triacrylate |

# 1. INTRODUCTION

## 1.1. Poly(β-amino ester)s

Poly(β-amino ester)s (PBAEs) constitute an important class of biomaterials due to their pH-sensitivity, high biocompatibility and biodegradability. They contain amine and ester groups at their main chains and are synthesized by aza-Michael addition of primary or secondary amines to di- or trifunctional acrylates without the need of catalysts or solvents (Figure 1.1). They are degradable under physiological conditions into small molecules like bis(β-aminoacid)s, diols and poly(acrylic acid)s. PBAEs find applications such as drug and gene delivery vehicles and tissue engineering scaffolds.

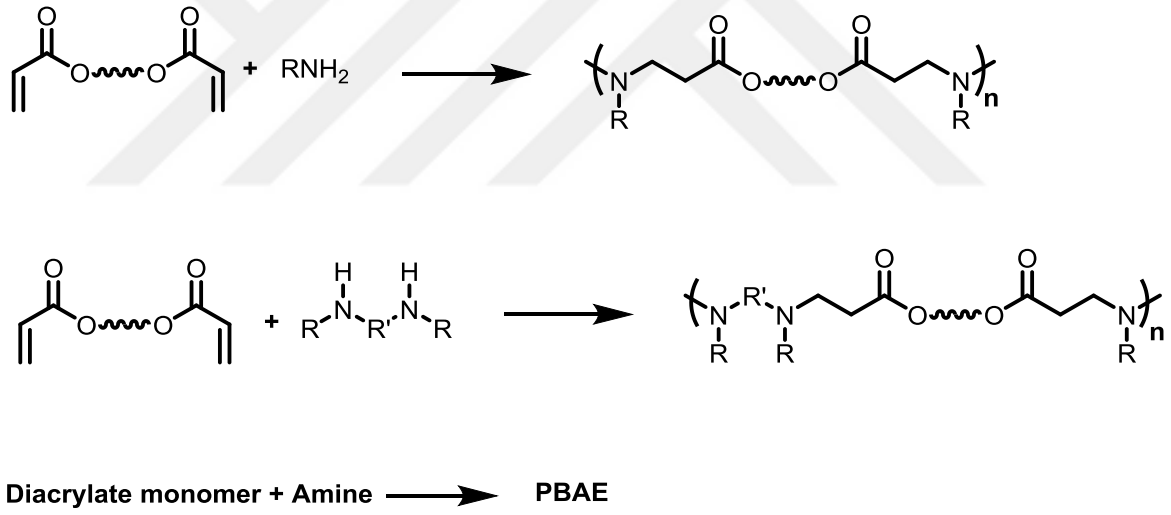


Figure 1.1. Synthesis of poly(β-amino ester)s.

### 1.1.1. Gene Delivery Applications

PBAEs are developed as non-viral gene delivery vehicles due to their ability to condense the negatively charged DNA into nanoparticles, to buffer the endosome leading to DNA escape and also their low cytotoxicity compared to polyethyleneimine (PEI) which is the widely studied polymer for gene delivery. The low degree of cytotoxicity is due to

their hydrolyzable structure avoiding the accumulation of positively charged high molecular weight polymers in cells.

Small modifications to the polymer end-capping molecules, tuning of polymer molecular weight and branching were shown to significantly affect the transfection efficacy and biocompatibility [1-8]. For example, a recent study showed that some end-modified PBAEs can deliver genes to primary glioblastoma cells with non-specific toxicity [1] (Figure 1.2).

These days, multi-drug resistance (MDR) effect is one of the main challenges in successful chemotherapy. An attempt to address this problem [2] utilized RNA interference and PBAE/RNA complex nanoparticles were prepared. It was illustrated that these complex systems could be applied as non-viral RNA carriers for reversing MDR.

Although gene therapy is important for treating specific acquired and inherited diseases, the lack of safe and efficient gene delivery systems remains as the major challenge. Since PBAEs have good properties in biosafety, DNA delivery efficiency and convenience in synthesis, they were coupled with low molecular weight PEI. PEI–PBAE showed significantly higher transfection efficiency with little cytotoxicity [3] (Figure 1.3).

A new class of PBAEs were synthesized by using the primary amine, 2-(pyridyldithio)-ethylamine [4]. Pyridylthio groups in the side chains of these polymers show fast reactivity with thiol ligands such as the thiol peptide RGDC which is a ligand specific to integrin receptors. Their complexes with DNA showed low cellular toxicity with medium transfection comparable to PEI.

Another study suggests a strategy to maintain intracellular DNA release as well as reduce polycation toxicity by controlling degradation using external triggers [5]. A library of mannosylated PBAEs with an increase in transfection capability both in vitro and in vivo was highlighted in [6]. Also, chemical modification at the termini of PBAEs with oligopeptides which are rich in amines, shows strong potential for future gene delivery

systems [7]. Ketal containing PBAE (KPAE), cleavable at the acidic pH of endosomal compartments was reported as a non-viral siRNA delivery system [8].

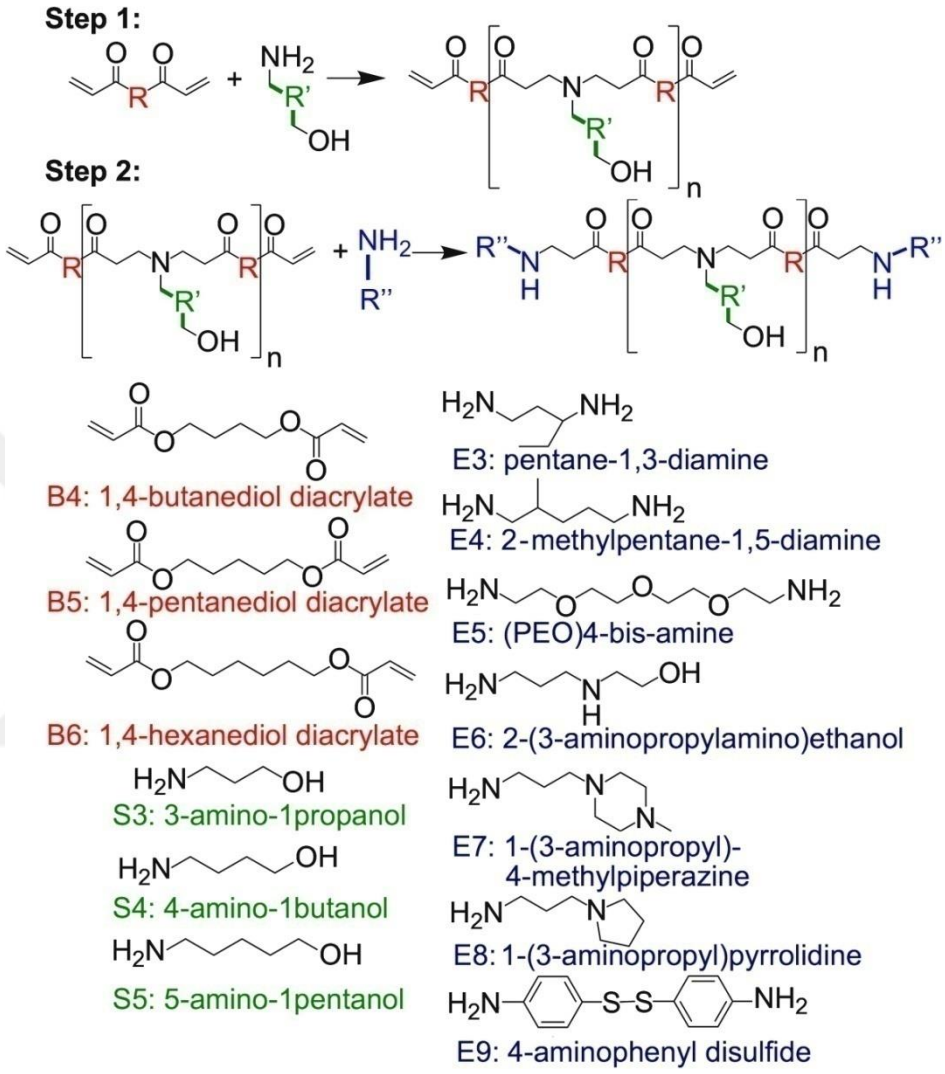


Figure 1.2. Synthesis of end-modified PBAEs [1].

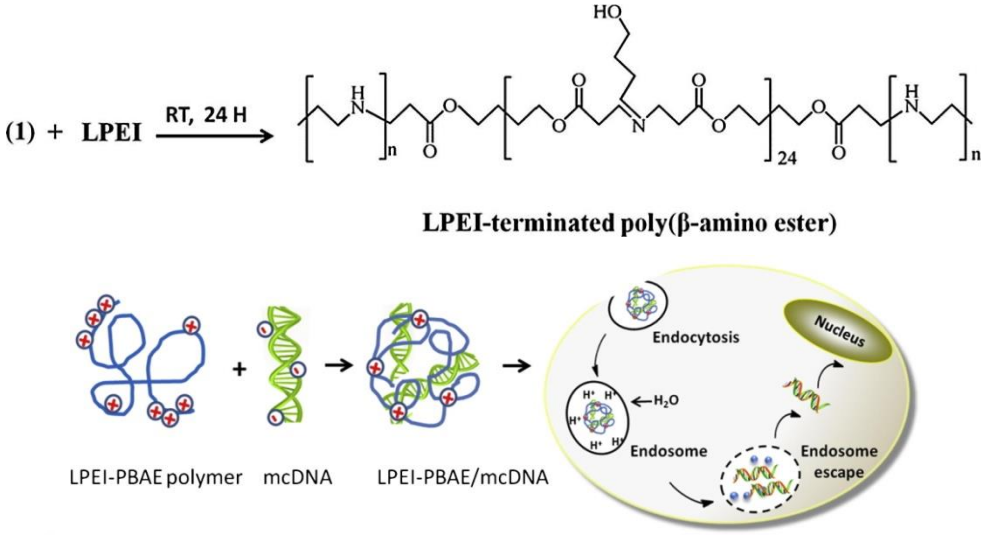


Figure 1.3. PEI terminated PBAE [3].

### 1.1.2. Drug Delivery Applications

Amphiphilic copolymers or nanoparticles of PBAEs are used for development of site-specific drug delivery systems. They have pH-dependent solubility and can be used to trigger release of drugs, oligonucleotides and plasmid DNA upon exposure to acidic environment. PBAEs are insoluble at physiological pH (7.4) due to their unprotonated structures, but become soluble when the pH of the solution is less than 6.5 due to their quaternized structures. This transition occurs over the range of extracellular and endosomal pH (7.4 and 5.0-6.5). Therefore the lower extracellular pH of tumor tissue compared to that of normal tissue has been used for drug delivery strategies [9-16].

The $pK_b$ values of PBAEs can be tuned across a broad range by changing the alkyl groups of the amines [9] (Figure 1.4). In general, PBAEs are the hydrophobic segment of amphiphilic copolymers while poly(ethylene glycol) (PEG) in the main [10-11] side chain constitutes the hydrophilic block [12-13]. For example, doxorubicin release was investigated by using pH-responsive polymeric micelles of MPEG-poly(β-amino ester) block copolymer [11] (Figure 1.5). Amphiphilic copolymers of PBAEs containing PEI were also designed for co-delivery of doxorubicin and RNA for effective therapy of drug resistant breast cancer [12].

PBAE hydrogel nanocomposites containing iron oxide and paclitaxel were investigated for chemotherapeutic and heat delivery (by induction in iron oxide particles via externally applied alternating magneting field) in the treatment of cancer. The main purpose of heating is to maintain hyperthermia, which means the heating of cancerous tissue up to 45 °C in order to increase efficiency of chemotherapy [13].

A PBAE was synthesized with piperazine and 1,4-butanediol diacrylate for application as a drug delivery matrix. The release of the drug was extended to over 10 days in DMF at 25 °C [14].

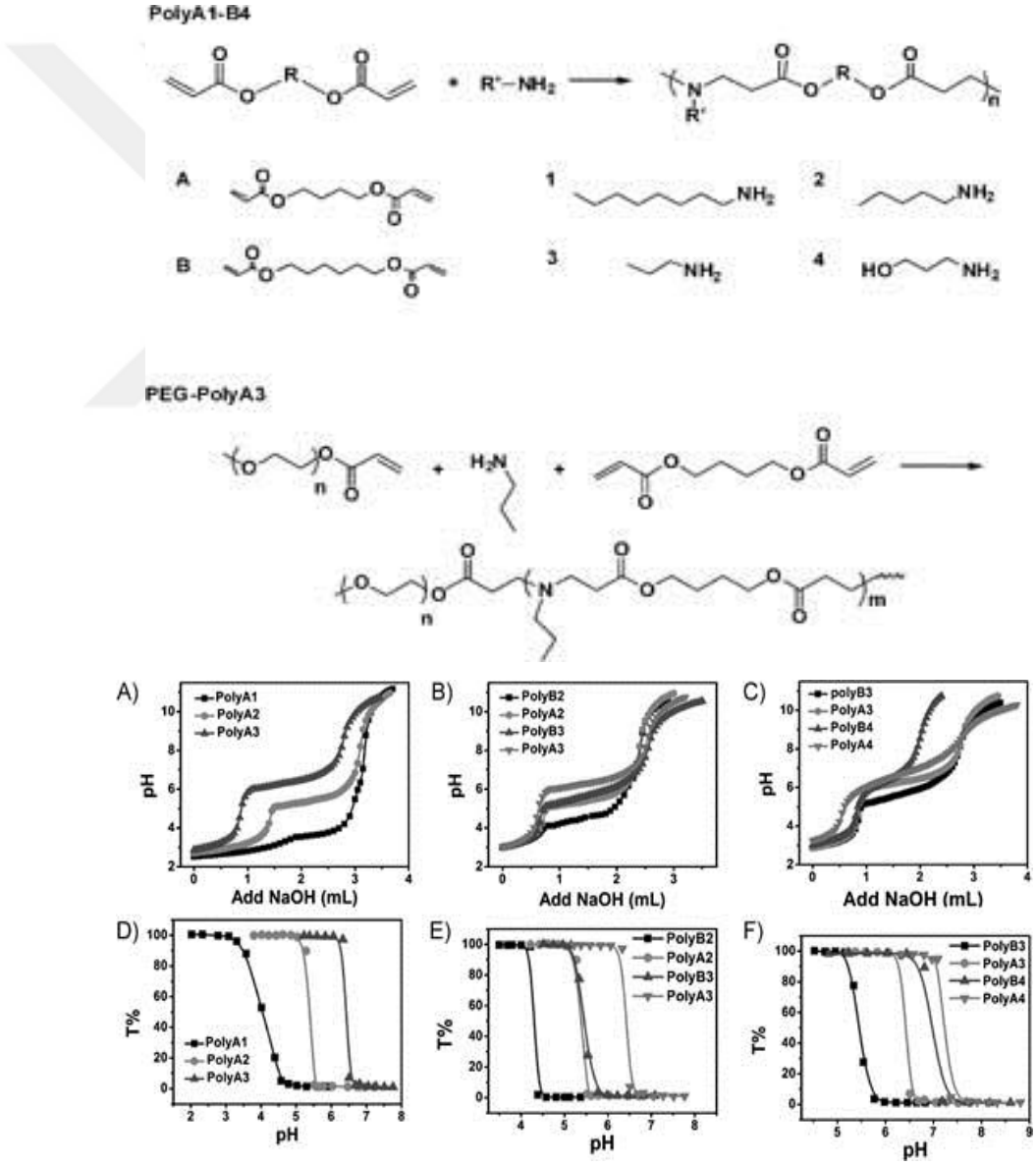


Figure 1.4. Preparation of PBAEs, PEG-PBAE block copolymers and titration curves of some of PBAEs [9].

Redox responsive polymers gained importance during recent years because of the overexpression of the reducing agent glutathione (GSH) in the tumor cells [15]. Dual redox- and pH-sensitive copolymeric micelles were prepared for intracellular doxorubicin delivery due to the fact that the tumor tissues show high reduction environment as well as low pH (Figure 1.6).

Also, redox and pH sensitive PBAE crosslinkers were used in the preparation of a protein encapsulated hydrogel. (Figure 1.7). They showed excellent controlled release in response to external conditions [16].

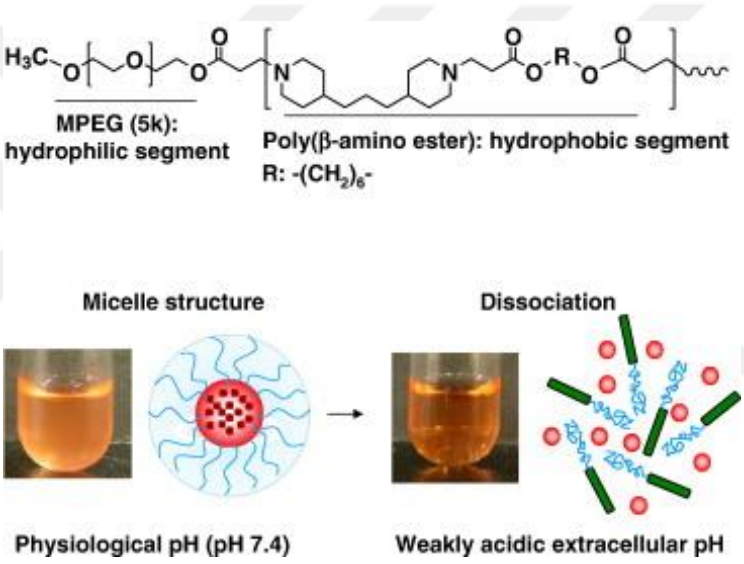


Figure 1.5. Structure of MPEG-PBAE block copolymer and dissociation of DOX-loaded micelles under physiological pH [11].

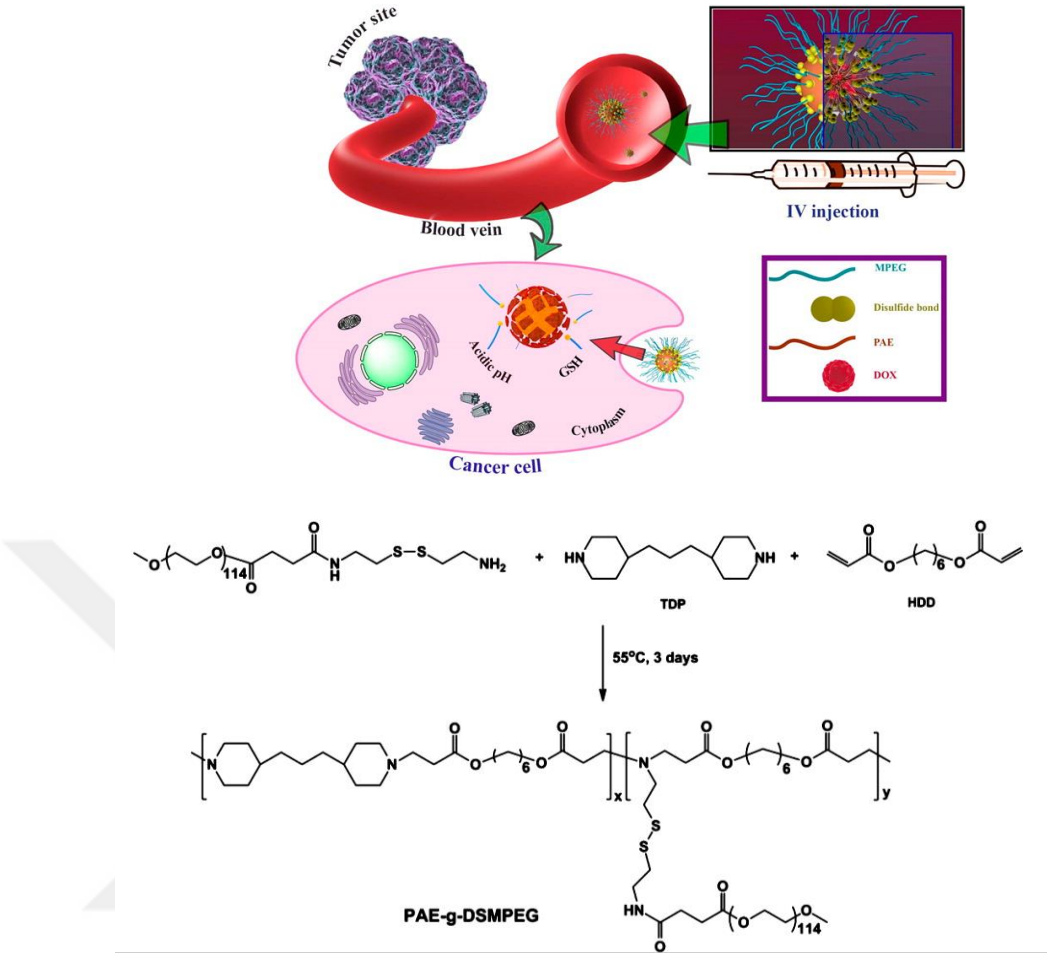


Figure 1.6. Dual redox- and pH-sensitive copolymeric micelles which are prepared for intracellular doxorubicin delivery [15].

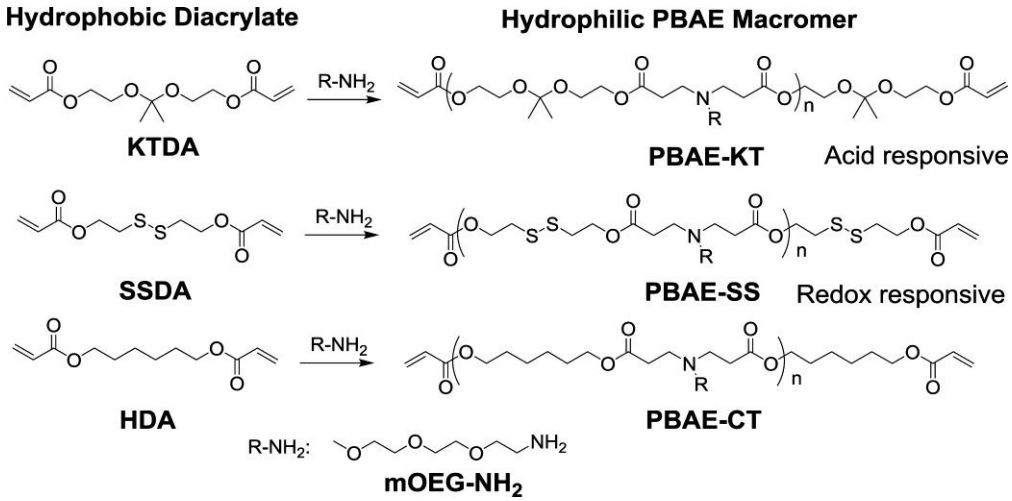


Figure 1.7. Synthesis of trigger-responsive PBAE crosslinkers [16].

### 1.1.3. Tissue Engineering Applications

Materials which show appropriate mechanical properties and degradation rates can be used for tissue engineering applications [17,18]. Degradation is essential in tissue engineering scaffolds because it prevents the necessity of second surgery. It may also aid in healing if the degradation rate is consistent with the cell penetration and tissue formation rate. Mechanical properties are important if the material is to be strong enough to bear the load of the tissue.

The polymer molecular weight and chain end groups of PBAEs can be easily controlled by adjusting the amine/diacrylate monomer ratio. Macromers with acrylate end groups can be easily prepared using acrylate/amine molar ratios of 1.4 to 1.1 [18]. Photopolymerization of macromers gives crosslinked and degradable networks which can be used as scaffolds for tissue engineering.

In literature, a library of PBAEs was created and the effect of the structure of acrylates and amines was investigated [17] (Figure 1.8). The polymers exhibited a wide range of degradation rates according to the hydrophilicity of the monomer. Polymers which contain hydrophilic ethylene glycol units degraded faster with respect to the other polymers (Figure 1.9).

The influence of macromer branching on network properties was investigated by adding a trifunctional monomer, trimethylolpropanetriacrylate [19].

The influence of molecular weight of macromer on network properties was investigated (Figure 1.10). It was found that the elastic moduli increase with increasing diacrylate/amine ratio. Also, it was found that mass loss correlates with a decrease in tensile modulus [18].

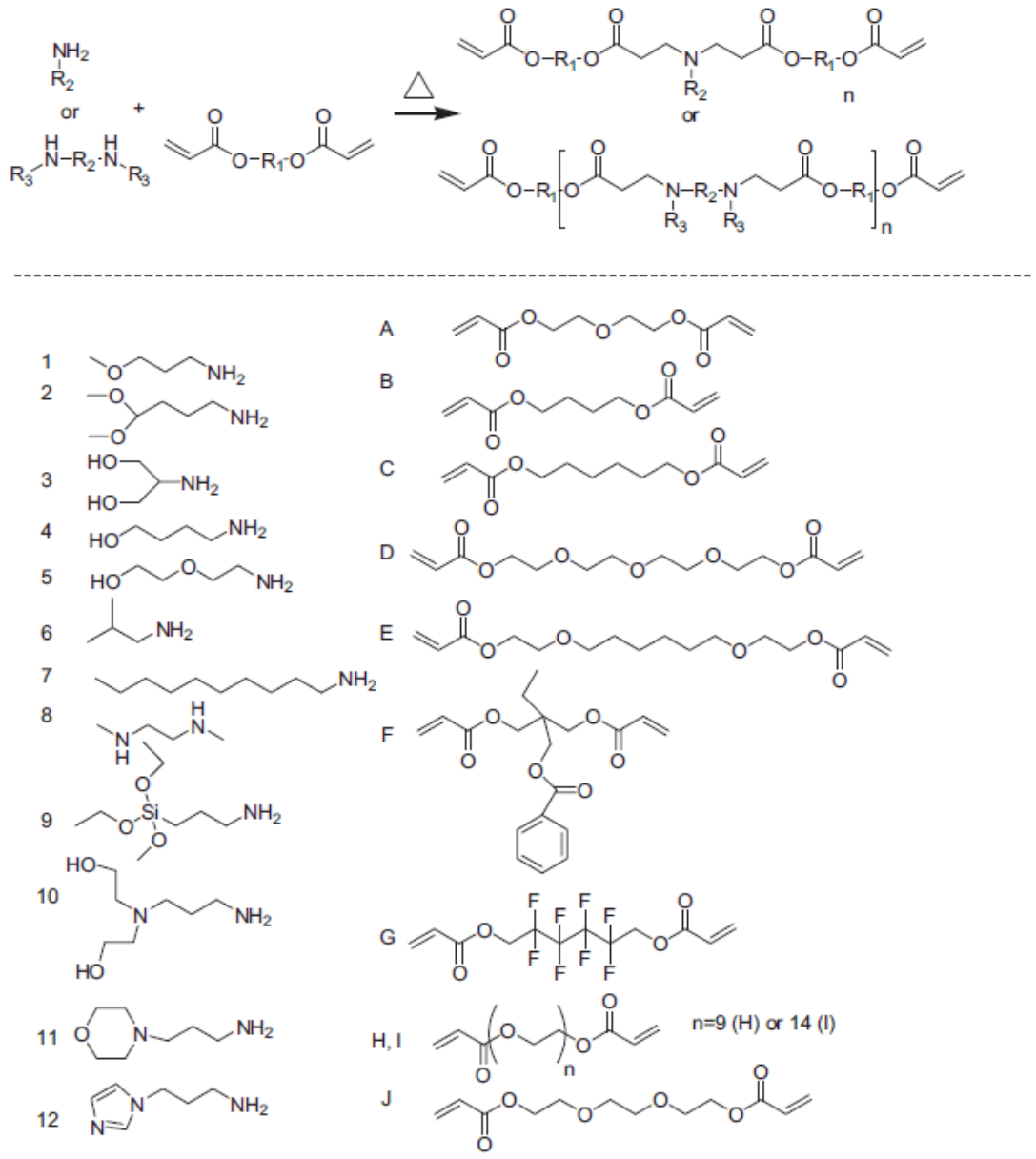


Figure 1.8. General synthesis scheme and the acrylates and amines used to produce a library of 120 photopolymerizable macromers [17].

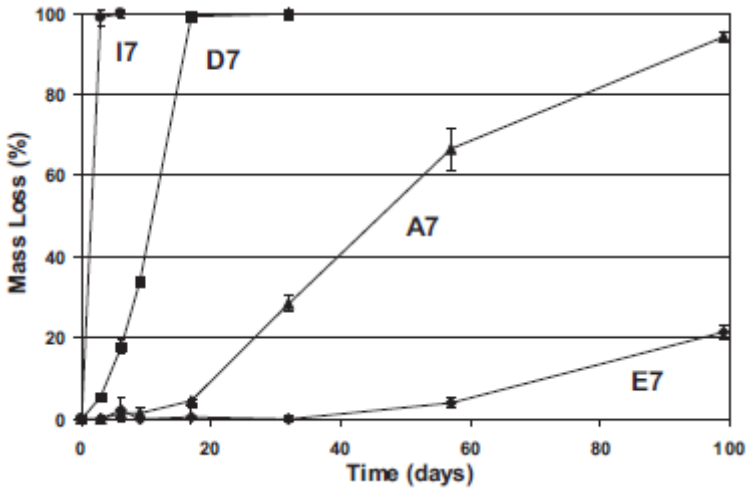


Figure 1.9. Degradation behavior of polymers synthesized from one amine and four acrylates [17].

Electrospun fibrous scaffolds with higher elastic modulus were developed for the engineering of numerous tissues [20,21]. As an alternative to free radical synthesis of PBAE hydrogels, one step method has been developed utilizing Michael addition of diacrylates and tetrafunctional primary amines [22] (Figure 1.11).

Thermosets based on a dual curing process, the aza-Michael reaction between multifunctional amine and acrylate monomers, and radical photopolymerization, are described for the preparation of materials with tailor-made mechanical and thermal properties [23]. PBAE crosslinkers were used for the synthesis of hydrogels (Figure 1.12) and the degradation properties of the hydrogels were compared to those crosslinked with PEGDA of similar molecular weights [24] (Figure 1.13).

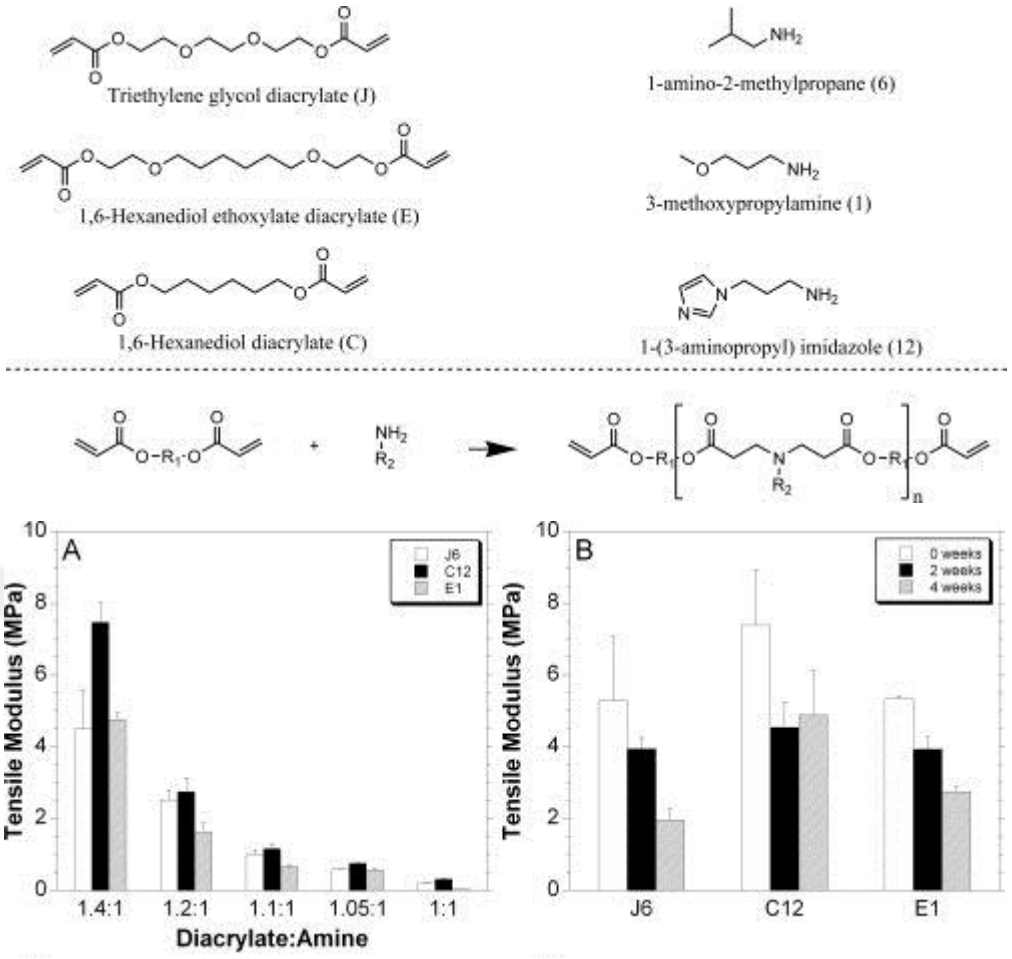


Figure 1.10. Effect of macromer molecular weight on tensile modulus [18].

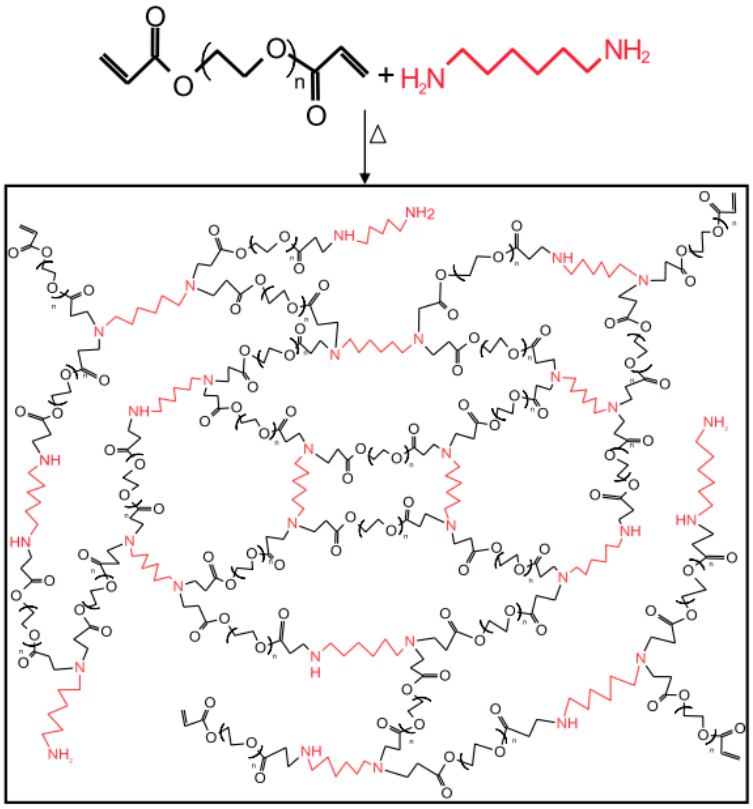

Figure 1.11. PBAEs synthesized from diacrylates and tetrafunctional primary amines [22].

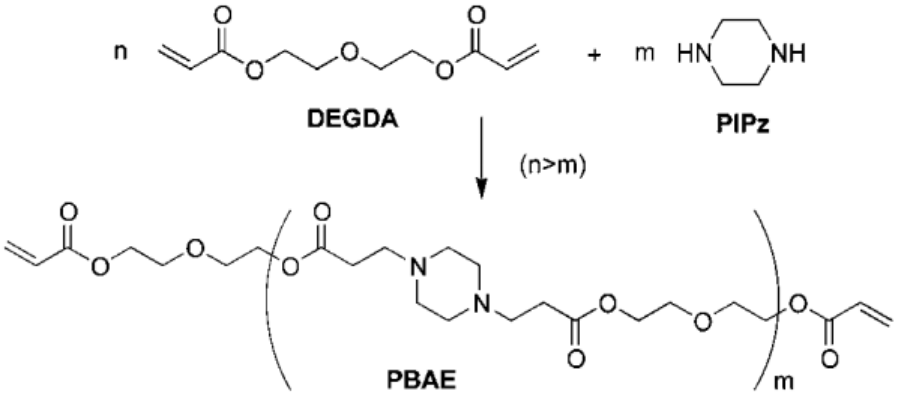


Figure 1.12. Polymer obtained from the synthesis of diacrylate and multifunctional amine [24].

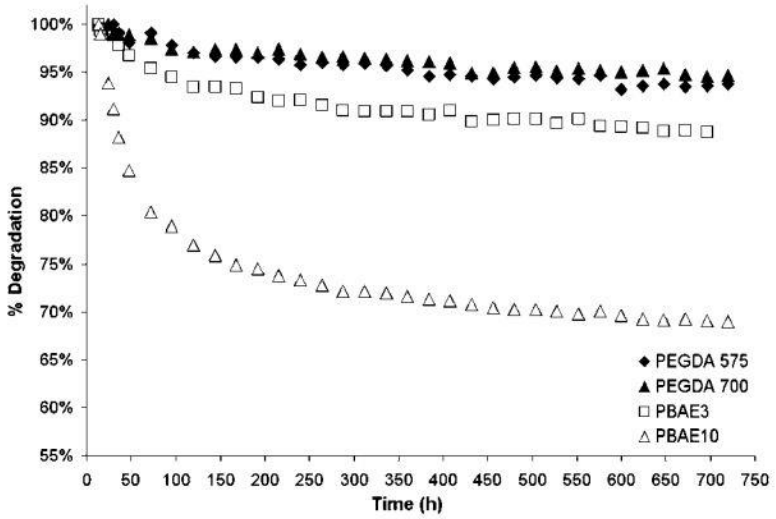


Figure 1.13. Degradation properties of the hydrogels [24].

## 1.2. Phosphorous Based Biomaterials

Recently phosphorus-based materials such as polyphosphates, polyphosphonates, polyphosphoesters, phosphonated and bisphosphonated poly(meth)acrylates have gained much attention as biomaterials [25]. Their important properties are biodegradability, hemocompatibility, protein adsorption resistance, and strong interactions with dentin, enamel and bone. Therefore one of the important application areas includes dental materials such as dental adhesives and composites. The phosphonic/phosphoric and bisphosphonic acid function leads to complex formation with calcium in hydroxyapatite (HAP) in dental tissues [26,27] (Figure 1.14). In recent years, phosphonic and bisphosphonic acid functionalized methacrylamides have been important due to their hydrolytic stability in oral environment [28, 29].

The same property is the basis of bone targeting systems for carrying bioactive molecules such as drugs and proteins or imaging agents for diagnostic applications [30,31] (Figure 1.15).

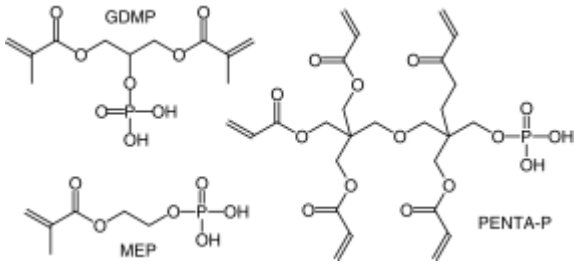


Figure 1.14. Self-etching dental adhesive monomers containing phosphoric acids [26].

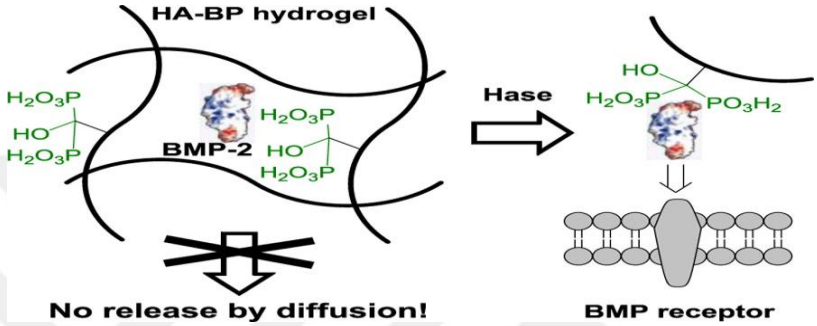


Figure 1.15. Bone targeting systems for carrying bioactive molecules [31].

Phosphorus-containing polymers have been shown to mineralize in vitro and in vivo such that they have a radioopacity similar to that of bone [32]. Therefore vinyl monomers containing phosphonate, phosphonic acid, phosphate, bisphosphonate and bisphosphonic acid groups were used for copolymerization [32,33]. A copolymer of vinyl phosphonic acid and acrylamide exhibited better proliferation, adhesion, differentiation, and ability to mineralize the polymer surface than pure polyacrylamide [34] (Figure 1.16). Hydrogels were prepared from phosphoester-containing poly(ethyleneglycol) for application to cartilage and bone tissue engineering [35] (Figure 1.17). Bisphosphonic acid containing materials were prepared for biomineralization [36,37]

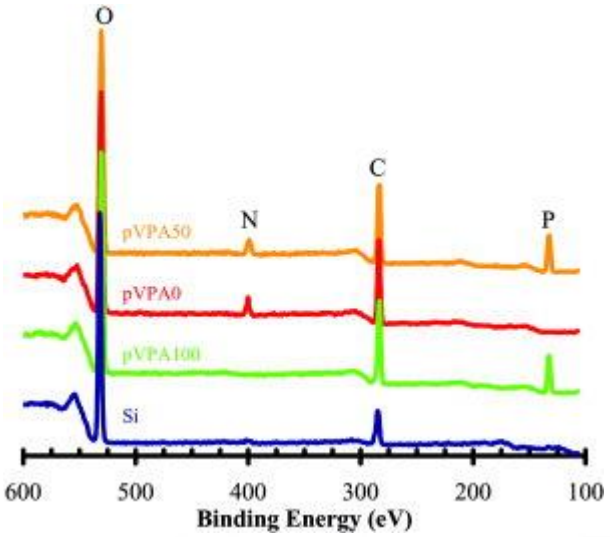


Figure 1.16. Binding energies of different materials [34].

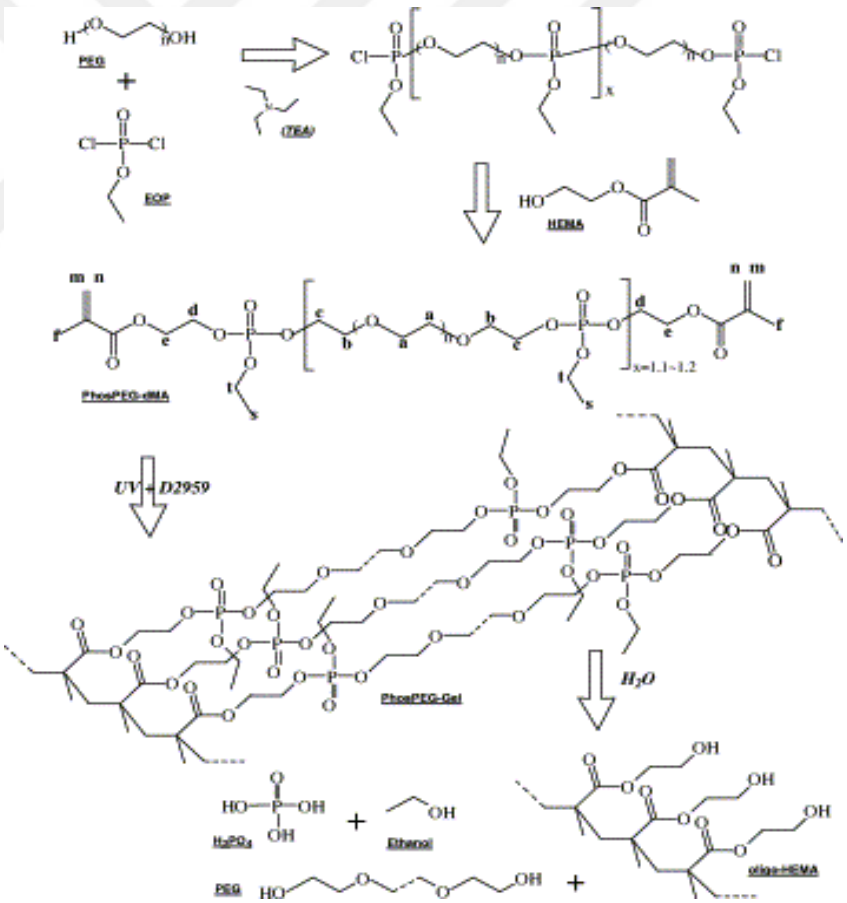


Figure 1.17. Hydrogels prepared from phosphoester-containing poly(ethyleneglycol) for bone cartilage and tissue engineering [35].

# 2. OBJECTIVES

The aim of this project is to synthesize new phosphonate-containing poly(β-amino ester) macromers and their network polymers to investigate the effects of attaching the phosphonate group and differences in the structure of the phosphonate groups in the macromer; on degradability and binding to tissues of the polymers. The materials' biocompatibility and biodegradability properties are expected to be improved due to the use of the phosphonate group.

# 3. EXPERIMENTAL WORK

## 3.1. Materials and Characterization

### 3.1.1. Materials

The following analytical-grade chemicals were obtained from commercial sources and used without any further purification: 1,6-hexane diol diacrylate (HDDA), poly(ethylene glycol) diacrylate (PEGDA, $M_n$=575), 1,4-butane diol diacrylate (BDDA), 1,6-hexanediol ethoxylatediacrylate (HDEDA), triethyleneglycoldiacrylate (TEGDA), trimethylolpropanetriacrylate (TMPTA), propyl amine (PA), diethyl vinylphosphonate, potassium phtalimide, 2,2-dimethoxy-2-phenylacetophenone (DMPA), propyl amine (PA), 1,6-dibromo hexane and all other reagents were obtained from Aldrich Chemical Co.; absolute ethanol and ammonia solution were purchased from Merck, hydrazine monohydrate was obtained from Alfa Aesar and triethylphosphite was purchased from Acros Organics.

Roswell Park Memorial Institute (RPMI) 1640 medium (with l-glutamine and 25 mM HEPES), trypsin-EDTA and penicillin-streptomycin were purchased from Multicell, Wisent Inc. (Canada). Fetal bovine serum was obtained from Capricorn Scientific GmbH (Germany). Phosphate buffered saline (PBS) tablets and thiazolyl blue tetrazolium bromide (MTT) were provided by Biomatik Corp. (Canada). Paraformaldehyde solution 4 % in PBS was obtained from Santa Cruz Biotechnology, Inc. (USA). 4′,6-diamidino-2-phenylindole (DAPI), fluorescein isothiocyanate (FITC)-labelled phalloidin and dimethyl sulfoxide (DMSO) Hybri-Max were purchased from Sigma (USA). 24-well (treated and non-treated) and 96-well PS plates (treated) were obtained from Nest Biotechnology Co. Ltd. (China). Human osteogenic sarcoma cell line Saos-2 was given as a gift from the Kavakli Lab (Koc University, Istanbul, Turkey) for this study.

### 3.1.2. Characterization

The proton nuclear magnetic resonance ($^1$H NMR) spectra (Varian Gemini 400 MHz) of macromers were obtained by using $CDCl_3$ as solvent. Fourier transform infrared (FTIR) spectra of macromers were recorded in a spectrometer NICOLET 6700, Thermo in the range of 4000–650 $cm^{-1}$. The molecular weights were determined by gel permeation chromatography (GPC) (Viscotek) with THF solvent using polystyrene standards.

## 3.2. Synthesis of Starting Materials

### 3.2.1. Synthesis of diethyl 2-aminoethylphosphonate (A1)

This amine was synthesized according to a literature procedure [38]. Ammonia (15 mL) was added to diethyl vinyl phosphonate (0.01 mol) at room temperature. After stirring for 3 days at room temperature, the reaction mixture was extractred with $CHCl_3$ (3 x 15 mL). The organic layer was dried over anhydrous $Na_2SO_4$, filtered and evaporated under reduced pressure. The residue was distilled under reduced pressure to give the pure product as a colorless liquid in 30% yield.

$^1$H-NMR (400 MHz, $CDCl_3$, TMS): $\delta$ = 1.32 ($CH_3$), 2.03 ($CH_2$-P), 2.87 ($CH_2$-N), 3.3 ($NH_2$), 4.11 ($CH_2$-O) ppm.

FT-IR (ATR): 3297 (N-H), 1162 (C-O), 1232 (P=O), 1026, 951 (P-O) $cm^{-1}$.

### 3.2.2. Synthesis of diethyl (6-amino hexyl) phosphonate (A2)

This amine was synthesized in three steps according to literature procedures [39,40]. 1,6-Dibromohexane (1.85 mL, 0.12 mol) was treated with potassium phtalimide at 140 °C for 24 hours. The reaction mixture was poured into chloroform, and the precipitate was removed by filtration. The addition of petroleum ether to the filtrate afforded N-(6-bromohexyl)phtalimide crystals.

$^1$H-NMR (400 MHz, $CDCl_3$, TMS): δ = 1.34 ($CH_3$), 1.44, 1.67, 1.84 ($CH_2$), 3.38 (N-$CH_2$), 3.64 (Br-$CH_2$), 7.70, 7.82 (Ar-CH) ppm.

FT-IR (ATR): 2962, 2935, 2860 ($CH_2$), 1721 (C=O), 1162 (C-O), 1260,1211 (Aryl $CH_2$), 1232 (P=O), 1026, 951 (P-O) $cm^{-1}$.

N-(6-Bromohexyl)phtalimide (0.5 g, 0.0016 mol) was added to triethylphosphite (1.34 g, 0.008 mol) slowly at room temperature. The mixture was refluxed for 12 hours, and then triethylphosphite were distilled out under reduced pressure (3 mm Hg) at 60 °C. The pure product, diethyl 6-phthalimidohexylphosphonate, was obtained as a yellow liquid in 70% yield.

$^1$H-NMR (400 MHz, $CDCl_3$, TMS): δ = 1.17 ($CH_3$), 1.34, 1.57 ($CH_2$),1.67 (P-$CH_2$), 3.71 (N-$CH_2$), 4.02 (O-$CH_2$), 7.63, 7.84 (Ar-CH) ppm.

FT-IR (ATR): 2935, 2862 ($CH_2$) , 1707 (C=O), 1162 (C-O), 1260,1211 (Aryl $CH_2$), 1238 (P=O), 1024, 954 (P-O) $cm^{-1}$.

Hydrazine monohydrate (0.5 g, 1mmol) was added to a solution of diethyl 6-phtalimido hexylphosphonate (0.036 g,0.1mmol) in ethanol (10 mL) at room temperature. The reaction mixture was stirred at room temperature for 12 hours. The precipitated solid was filtered and identified as phtalyl hydrazide. The solvent was removed under reduced pressure and the crude product was purified by column chromatography on a silica gel using a gradient of ($CHCl_3$/MeOH (9:1)). After evaporation of the solvent diethyl 6-aminohexyl phosphonate was obtained as a yellow liquid.

$^1$H-NMR (400 MHz, $CDCl_3$, TMS): δ = 1.22 ($CH_3$), 1.31, 1.52, 1.61, ($CH_2$), 1.69 (O=P-$CH_2$), 2.60 (N-$CH_2$),4.01 (O-$CH_2$) ppm.

FT-IR (ATR): 2935, 2862 ($CH_2$), 1707 (C=O), 1162 (C-O), 1260,1211 (Aryl $CH_2$), 1238 (P=O), 1024, 954 (P-O) $cm^{-1}$.

### 3.3. Synthesis of poly(β-amino ester) macromers

The diacrylates (HDDA, PEGDA, HDEDA, BDDA and TEGDA) and amines (PA, A1 and A2) were mixed at molar ratios of 1.1:1 and 1.2:1 in 10 mL scintillation vials at 90 °C 24h while stirring. The viscous macromers were washed with petroleum ether to remove unreacted diacrylates and secondary amines produced, and dried under reduced pressure.

*HDDA-A1*

$^1$H-NMR (400 MHz, $CDCl_3$, TMS): δ = 1.26 ($CH_3$), 1.34 ($CH_2$), 1.58 ($CH_2$), 1.85 ($CH_2$-P), 2.40 ($CH_2$-C=O), 2.60 ($CH_2$-N), 2.70 ($CH_2$-N), 3.98 ($CH_2$-O), 4.03 ($CH_2$-O), 4.08 ($CH_2$-O-P), 5.75 (CH=CH-*H*), 6.07 (C*H*=$CH_2$), 6.35 (CH=CH-*H*) ppm.

FTIR (ATR): 2981 (C-H), 1721 (C=O), 1635 (C=C), 1230 (P=O), 1026, 951 (P-O) $cm^{-1}$

*HDDA-PA*

$^1$H-NMR (400 MHz, $CDCl_3$, TMS): 0.85 ($CH_3$), 1.39 ($CH_2$), 1.42 ($CH_2$), 1.62 ($CH_2$), 2.35 ($CH_2$-N), 2.45 ($CH_2$-C=O), 2.75 ($CH_2$-N), 4.04 ($CH_2$-O), 4.14 ($CH_2$-O), 5.80 (CH=CH-*H*), 6.10 (C*H*=$CH_2$), 6.40 (CH=CH-*H*) ppm.

FTIR (ATR): 2935 (C-H), 1721 (C=O), 1613 (C=C) $cm^{-1}$.

*PEGDA-A1*

$^1$H-NMR (400 MHz, $CDCl_3$, TMS): δ = 1.29 ($CH_3$), 1.88 ($CH_2$-P), 2.45 ($CH_2$-N), 2.47 ($CH_2$-C=O), 2.74 ($CH_2$-N), 3.63 ($CH_2$-O), 3.73 ($CH_2$-O), 4,30 ($CH_2$-O), 5.82 (CH=CH-*H*), 6.09 (C*H*=$CH_2$), 6.40 (CH=CH-*H*) ppm.

FTIR (ATR): 2867 (C-H), 1724 (C=O), 1635 (C=C), 1232 (C-O), 1025, 950 (P-O) $cm^{-1}$.

*PEGDA-PA*

$^1$H-NMR (400 MHz, $CDCl_3$, TMS): $\delta$ = 0.56 ($CH_3$), 1.14 ($CH_2$), 1.22 ($CH_2$), 2.05 ($CH_2$-N), 2.15 ($CH_2$-C=O), 2.45 ($CH_2$-N), 3.36 ($CH_2$-N), 3.92 ($CH_2$-O), 4.02 ($CH_2$-O), 5.55 (CH=CH-*H*), 5.85 (C*H*=$CH_2$), 6.15 (CH=CH-*H*) ppm.

FTIR (ATR): 2869 (C-H), 1721 (C=O), 1635 (C=C) $cm^{-1}$.

*HDEDA-A1*

$^1$H-NMR (400 MHz, $CDCl_3$, TMS): $\delta$ = 1.31 ($CH_3$), 1.56 ($CH_2$-$CH_2$), 1.65 ($CH_2$-$CH_2$), 1.89 ($CH_2$-P), 2.45 ($CH_2$-C=O), 2.75 ($CH_2$-N), 3.44 ($CH_2$-O), 3.63 ($CH_2$-O), 4.07 ($CH_2$-O-P), 4.20 ($CH_2$-$CH_2$-O), 4.29 (O-$CH_2$), 5.80 (CH=CH-*H*), 6.14 (C*H*=$CH_2$), 6.38 (CH=CH-*H*).

FTIR (ATR): 2935 (C-H), 1725 (C=O), 1636 (C=C), 1230 (P=O), 1024, 957 (P-O) $cm^{-1}$.

*BDDA-A1*

$^1$H-NMR (400 MHz, $CDCl_3$, TMS): $\delta$ = 1.30 ($CH_3$), 1.70 ($CH_2$-$CH_2$), 1.90 ($CH_2$-P), 2.44 ($CH_2$-C=O), 2.72 ($CH_2$-N), 2.74 ($CH_2$-N), 4.07 (O-$CH_2$), 4.17 ($CH_2$-O), 5.80 (C=CH-*H*), 6.08 (C*H*=$CH_2$), 6.38 (C=CH-*H*) ppm.

FTIR (ATR): 2962 (C-H), 1723 (C=O), 1635 (C=C), 1240 (P=O), 1023, 955 (P-O) $cm^{-1}$.

*TEGDA-A1*

$^1$H-NMR (400 MHz, $CDCl_3$, TMS): $\delta$ = 1.30 ($CH_3$), 1.87 ($CH_2$-P), 2.44 ($CH_2$-C=O), 2.72 (N-$CH_2$), 2.76 (N-$CH_2$) 3.65 ($CH_2$-O), 3.68 ($CH_2$-O), 4.07 ($CH_2$-O), 4.19 ($CH_2$-O), 4.30 ($CH_2$-O), 5.82 (CH=CH-*H*), 6.12 (C*H*=$CH_2$), 6.41 (CH=CH-*H*) ppm.

FTIR (ATR): 2962 (C-H), 1720 (C=O), 1635 (C=C), 1232 (P=O), 1023, 955 (P-O) $cm^{-1}$.

*PEGDA-A2*

$^1$H-NMR (400 MHz, $CDCl_3$, TMS): δ = 1.30 ($CH_3$), 1.87 ($CH_2$-P), 2.44 ($CH_2$-C=O), 2.72 (N-$CH_2$), 2.76 (N-$CH_2$) 3.65 ($CH_2$-O), 3.68 ($CH_2$-O), 4.07 ($CH_2$-O), 4.19 ($CH_2$-O), 4.30 ($CH_2$-O), 5.82 (CH=CH-*H*), 6.12 (C*H*=$CH_2$), 6.41 (CH=CH-*H*) ppm.

FTIR (ATR): 2867 (C-H), 1725 (C=O), 1639 (C=C), 1247 (P=O), 1097, 952 (P-O) $cm^{-1}$.

*HDDA-A2*

$^1$H-NMR (400 MHz, $CDCl_3$, TMS): δ = 1.28 ($CH_3$), 1.37 ($CH_2$), 1.48 ($CH_2$), 1.54 ($CH_2$), 1.67 ($CH_2$), 2.49 ($CH_2$-C=O), 2.82 (N-$CH_2$), 2.83 (N-$CH_2$),3.61 ($CH_2$-O), 4.04 ($CH_2$-O), 4.19 ($CH_2$-O), 4.28 ($CH_2$-O), 5.78 (CH=CH-*H*), 6.14 (C*H*=$CH_2$), 6.38 (CH=CH-*H*) ppm.

FTIR (ATR): 2861 (C-H), 1725 (C=O), 1635 (C=C), 1232 (P=O), 1023, 955 (P-O) $cm^{-1}$.

### 3.4. Synthesis of branched poly(β-amino ester) macromers

The diacrylates (PEGDA and BDDA), a triacrylate (TMPTA) and an amine (A1) were mixed at diacrylate: triacrylate ratios of 90:10 while holding the molar ratio of acrylate to amine constant (1.2:1) in scintillation vials at 90 °C overnight while stirring. The viscous macromers were washed with petroleum ether to remove unreacted amines and dried under reduced pressure.

PEGDA-TMPTA-A1

$^1$H-NMR (400 MHz, $CDCl_3$, TMS): δ = 1.29 ($CH_3$), 1.84 ($CH_2$-P), 2.43 ($CH_2$-N), 2.72 (O=C-$CH_2$), 3.62 ($CH_2$-O), 3.70 ($CH_2$-N), 4.04 ($CH_2$-O), 4.19 (O=C-O), 4.27 ($CH_2$-O), 5.79 (C=$CH_2$), 6.12 (CH=$CH_2$), 6.41 (C=$CH_2$) ppm.

FTIR (ATR): 2962 (C-H), 1725 (C=O), 1635 (C=C), 1184 (C-O), 1257 (P=O), 1023, 955 (P-O) $cm^{-1}$.

BDDA-TMPTA-A1

$^{1}$H-NMR (400 MHz, $CDCl_3$, TMS): $\delta$ = 1.30 ($CH_3$), 1.67 ($CH_2$), 1.89 ($CH_2$-P-), 2.46 ($CH_2$-N-), 2.73 (O=C-$CH_2$-), 4.02 ($CH_2$-O), 4.15 ($CH_2$-O), 5.81 (C=$CH_2$), 6.07 (CH=$CH_2$), 6.38 (C=$CH_2$) ppm.

FTIR (ATR): 2969 (C-H), 1722 (C=O), 1635 (C=C), 1181 (C-O), 1250 (P=O), 1023, 955 (P-O) $cm^{-1}$.

### 3.5. Synthesis of network polymers

The macromers were mixed with the photoinitiator (DMPA, dissolved in 1wt% methylene chloride) and the solvent was removed under reduced pressure. The macromer/initiator mixture was placed into a Teflon mold (5 mm diameter x 0.25 cm thickness), covered with a mylar film and polymerized with exposure to UV light (365 nm) for 30 min. The polymer samples were weighed and placed in ethanol for 24 h to remove unreacted macromers and initiators. After drying in a vacuum oven for several days until constant weight, gel samples were weighed. The percentage of gelation was calculated according to the following formula:

$$Gelation\ \% = \left(\frac{Weight\ After\ Polymerization}{Weight\ After\ Washing\ with\ EtOH\ and\ Drying}\right) \times 100 \qquad (3.1)$$

### 3.6. Photopolymerization

The photoinitiator (DMPA) was added to the macromers at a concentration of 1% (w/w) by the addition of a 10% (w/v) solution of DMPA in methylene chloride and solvent was removed in a vacuum desiccator overnight. The polymerization behavior was monitored using a real-time FTIR-ATR spectroscopy. A drop of the macromer/initiator solution was placed directly on diamond ATR, covered with a mylar film and exposed to UV-irradiation with an Omnicure 1000 W mercury arc lamp at 320-500 nm. The conversion profiles were calculated from the decay of the absorption bands of the double bond peak at 1635 $cm^{-1}$ with respect to the C=O peak at 1721 $cm^{-1}$, using peak height.

$$DC\ \% = \left(1 - \frac{Abs_{1635}^{sample}/Abs_{1721}^{sample}}{Abs_{1635}^{monomer}/Abs_{1721}^{monomer}}\right) \times 100 \quad (3.2)$$

### 3.7. Degradation

Degradation studies were carried out using the polymer samples as prepared above. The gel samples were submerged in PBS solution and placed on an orbital shaker at 37 °C. At each time point, samples were removed, dried, and weighed to determine the mass loss. Degradation % calculated according to the following formula:

$$Degradation\ \% = \left(\frac{Initial\ Weight - Final\ Weight}{Initial\ Weight}\right) \times 100 \quad (3.3)$$

### 3.8. In Vitro Cytotoxicity Assay

The in vitro cytotoxicity of degradation products were assessed using colorimetric MTT metabolic activity assay. SaOS-2 cells were grown in RPMI 1640 complete medium supplemented with 10 % FBS and 1 % penicillin–streptomycin antibiotic solution, at 37 °C in an atmosphere of 5 % CO2 at a density of 1x104 cells/well in 96 well plates. The medium was removed next day and cells were exposed to fresh medium with different concentration of degradation products in PBS (5-250 μg/mL) for 24 h. Finally, the medium in each well was replaced with 200 μL complete medium containing 0.25 mg MTT which forms purple formazan as a result of mitochondrial activity of viable cells. After 4 hours of incubation, ethanol: DMSO (1:1 v/v) solution was added to each well to dissolve the formazan crystals and the absorbance intensity at 600 nm was recorded with a reference wavelength of 630 nm by a microplate reader (BioTek ELx800 Absorbance Microplate Reader) [41]. The cell viability percentage relative to the untreated cells (100 % viability) was calculated according to the formula:

$$\%viability = \frac{Asample}{Acontrol} x100 \ \ (n = 4) \quad (3.4)$$

### 3.9. In Vitro Cell Interaction Studies

Macromers dissolved in ethanol at a ratio of 1:2 (w/v macromer:EtOH) were added to non-treated 24-well plates to obtain thin films on each well (100 μL). The ethanol was allowed to evaporate and plates were exposed to ultraviolet light for 30 mins. Cured films were incubated with ethanol three times for 4 h to remove the unreacted macromers. The plates were sterilized by exposure to UV light in a laminar flow hood for 1 h. Extra washing steps were performed with PBS and complete medium for 1 h in an incubator. SaOS-2 cells were seeded in hydrogel containing plates at a concentration of $5x10^4$ cells per well in RPMI complete medium and cultured for 24 h. For microscopy image analysis, the cells were fixed with 4% paraformaldehyde for 20 minutes at room temperature after being washed with PBS three times. Fixed cells were counterstained with DAPI (nucleus staining) and FITC-labelled phalloidin for intracellular actin staining according to manufacturer's protocol. 1 mL of PBS was placed in each well to keep the cells against air-drying. Images were taken using an Inverted Life Science Microscope (Olympus-Xcellence RT Life Science Microscopy) [42]. Nucleus and actin staining were visualized by appropriate filter sets: for DAPI: $\lambda_{exc}$: 352-402 nm and λem: 417-477 nm; for FITC: $\lambda_{exc}$: 490 nm and $\lambda_{em}$520 nm. Control cells were cultured in treated 24-well plates and same steps were repeated. ImageJ analysis program was used to process the recorded images [43].

### 3.10. Statistical Analysis

Kruskall–Wallis one-way analysis of variance followed by multiple Dunn's comparison test or Mann-Whitney test of GraphPad Prism 6 software package (GraphPad Software, Inc., USA) was applied for statistical analysis. Values were reported as mean values ± standard deviation (S.D.). All tests were two-tailed and P value was defined as less than 0.05.

# 4. RESULTS AND DISCUSSION

## 4.1. Synthesis of amines

In this work three primary amines were used as starting materials for the synthesis of PBAE macromers (Figure 4.1).

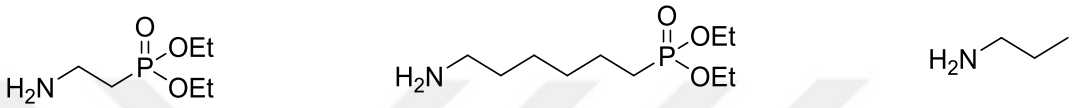


A1 A2 PA

Figure 4.1. Structures of amines.

The first amine (diethyl 2-aminoethylphosphonate) (A1) was synthesized from the reaction of diethyl vinyl phosphonate and ammonia [38] (Figure 4.2). In the $^{1}$H-NMR spectrum of this amine, we observed peaks at 2.03, 2.87 and 4.11 ppm due to methylene protons adjacent to phosphorous, nitrogen and oxygen (Figure 4.3).

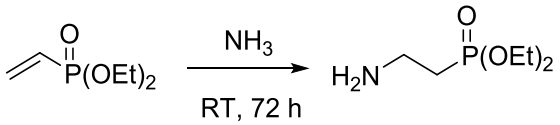


Figure 4.2. Synthesis of A1 [38].

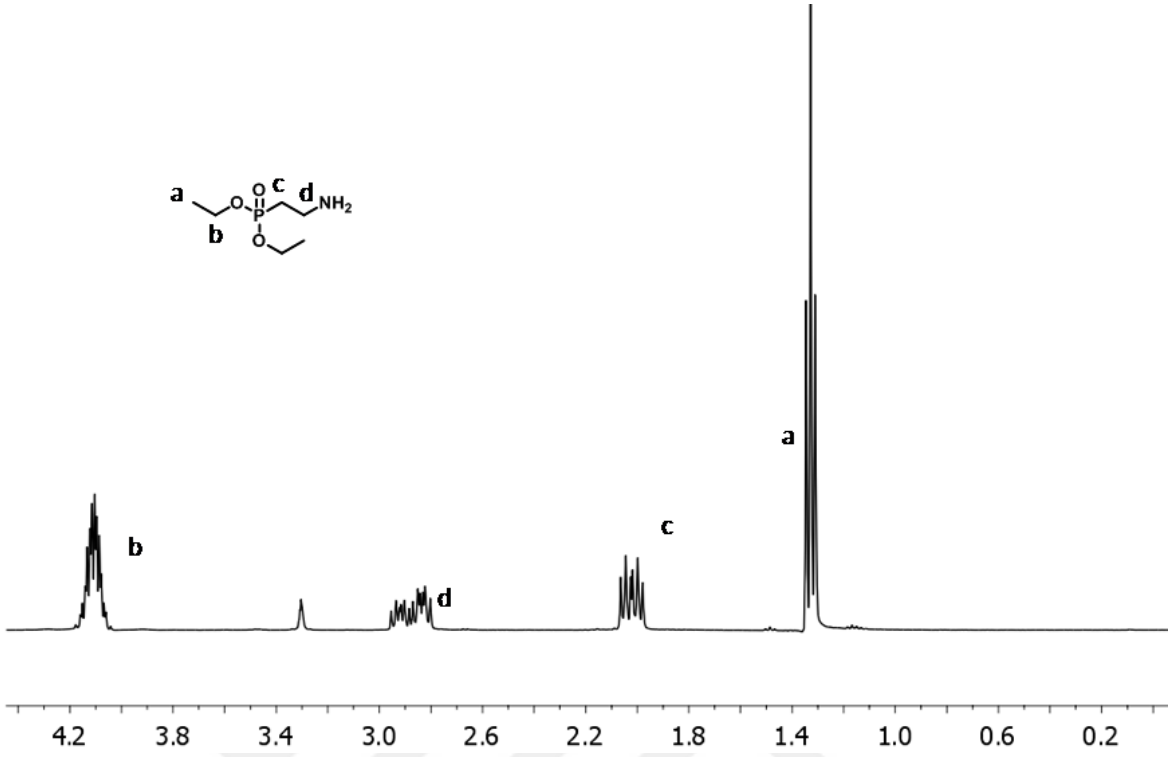


Figure 4.3. $^{1}$H-NMR spectrum of A1.

The second amine, diethyl (6-amino hexyl) phosphonate (A2), was synthesized in three steps: i) reaction of 1,6-dibromohexane with potassium phtalimide to give N-(6-bromohexyl)phtalimide; ii) synthesis of diethyl 6-phthalimidohexylphosphonate from reaction of N-(6-bromohexyl)phtalimide with triethylphosphite; iii) conversion of diethyl 6-phthalimidohexylphosphonate to diethyl (6-amino hexyl) phosphonate with hydrazine hydrate in ethanol [39,40] (Figure 4.4).

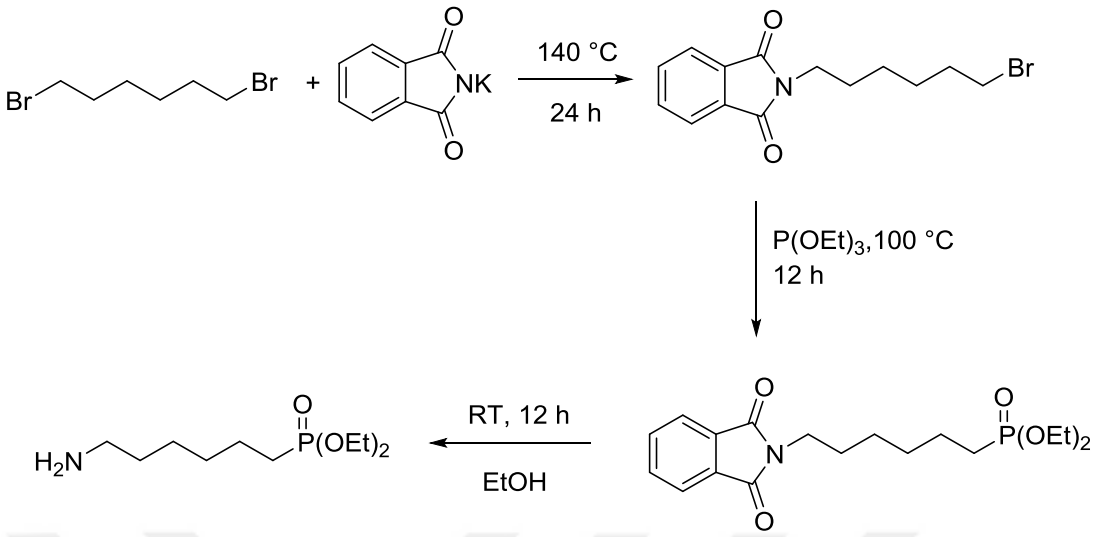


Figure 4.4. Synthesis of A2 [39,40].

In the $^{1}$H-NMR spectrum of the first intermediate, N-(6-bromohexyl)phtalimide, we observed aromatic protons around 7.5-8.5 ppm, methylene protons attached to nitrogen and bromine at 3.38 and 3.64 ppm and other methylene protons between 1.44 and 1.84 ppm (Figure 4.5). $^{1}$H-NMR spectrum of diethyl 6-phtalimidohexylphosphonate confirmed its structure (Figure 4.6). $^{1}$H-NMR spectrum of the final product, A2 (diethyl (6-amino hexyl) phosphonate), shows methyl protons at 1.22 ppm, methylene adjacent to nitrogen at 2.60 ppm and methylene attached to oxygen is at 4.01 ppm (Figure 4.7).

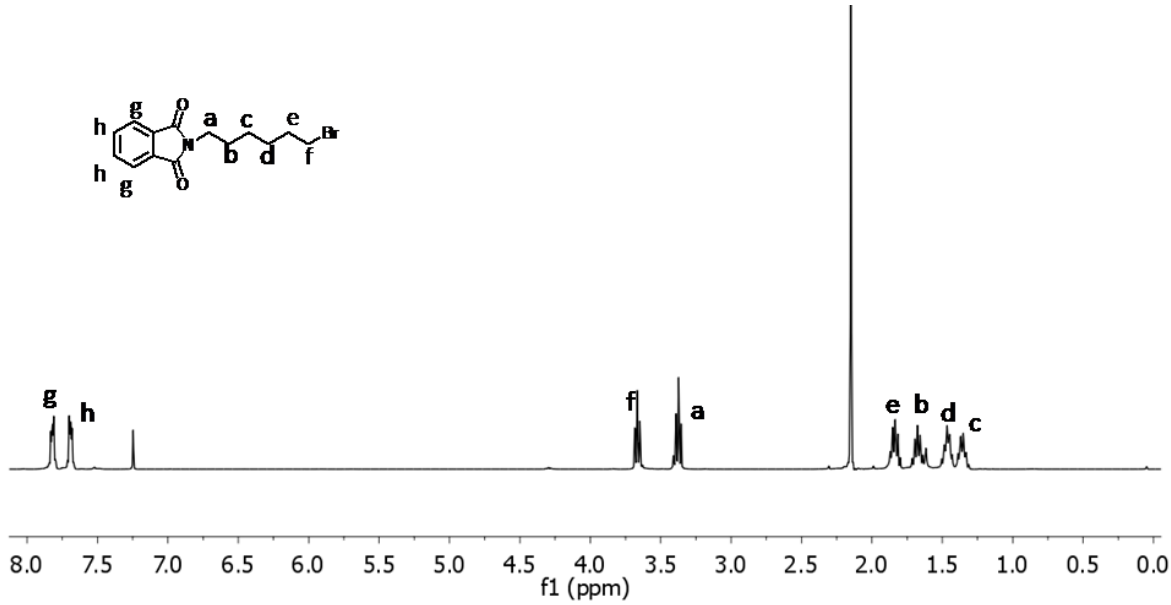


Figure 4.5. [1]H-NMR spectrum of N-(6-bromohexyl) phtalimide.

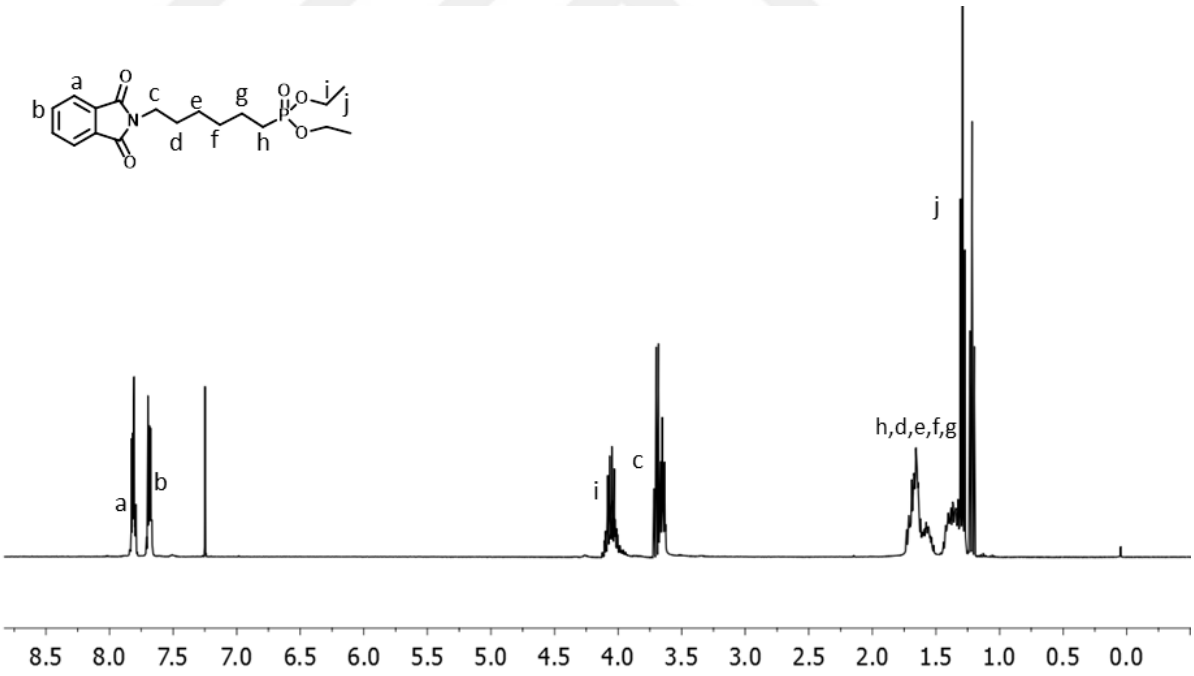


Figure 4.6. [1]H-NMR spectrum of diethyl 6-phthalimidohexylphosphonate.

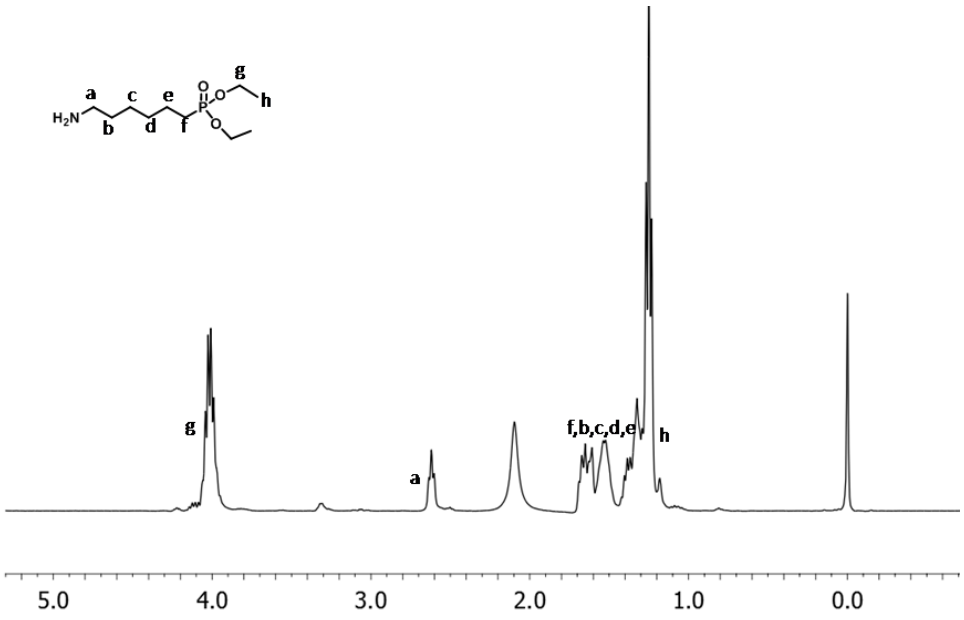


Figure 4.7. $^{1}$H-NMR spectrum of diethyl (6-amino hexyl) phosphonate.

## 4.2. Synthesis of PBAE macromers

Novel injectable and biodegradable diacrylate terminated phosphonated-poly(*β*-amino ester) macromers were produced by the aza-Michael condensation of primary amines (PA, A1 and A2) to diacrylates (HDDA, PEGDA, HDEDA, TEGDA and BDDA) (Figure 4.8) without any catalyst and solvent. Diacrylate to amine molar ratio which controls the extent of polymerization was varied at 1.1 and 1.2 and the reactions were completed in 12 h at 90 °C. It was observed that the reactions at lower temperatures (70 °C) were slow and took longer periods (72 h). We also synthesized branched macromers to investigate the effect of macromer branching on network properties. They were synthesized by adding a trifunctional monomer (TMPTA) to diacrylates (90:10 mol%) while the diacrylate to amine ratio is maintained at 1.2:1. The macromers were washed with petroleum ether or ether to remove unreacted starting materials or monoaddition products. The macromers were obtained as colorless to yellow in color in good yields (75%). Since these macromers were liquids at room temperature they can be used as injectable polymers. Except PEGDA-based macromers they were insoluble in water but soluble in most common organic solvents such as methylene chloride, THF, ethanol (Table 1). They are soluble in water at reduced pH.

The macromers were characterized by their spectroscopic (IR, $^1$H NMR) data. $^1$H NMR spectra show the persistence of acrylate peaks and appearance of complex peaks due to methylene attached to phosphorus at 1.85 ppm (Figure 4.9-4.18). Also the peaks due to methylenes attached to carbonyl, nitrogen and oxygen were observed at 2.40, 2.60-2.70 and 3.98-4.08 ppm. The area of acrylate peaks at 6.4, 6.0, and 5.8 ppm decreased with decreasing diacrylate to amine ratios from 1.2 to 1.1, indicating higher MMWs of the macromers, as expected (Figure 4.10). The average number of repeat units (n) which can be correlated with the number average molecular weight was calculated using $^1$H NMR, by integrating acrylate protons (5.7-6.4 ppm) with respect to methylene protons attached to C=O protons (2.4 ppm) or methyl protons (0.85-1.30 ppm) (Table 2). This technique could not be used for the branched system since the functionality of the macromers were not known. According to $^1$H-NMR results, A1-based macromers have slightly lower number of repeat units compared to PA-based macromers. This finding can be explained by the sterically hindered structure of A1 due to phosphonate group.

The molecular weights of polymers were also determined by organic phase (THF) gel permeation chromatography (GPC). Polymer molecular weights ($M_n$) were ca. 1000-3000, relative to polystyrene standards (Table 3). Molecular weight distributions for these macromers were monomodal with polydispersity indices (PDI) of ca. 1.2 – 1.8. These results are roughly in agreement with those obtained with $^1$H NMR spectroscopy.

The FTIR spectrum of macromers shows strong peaks at around 1721, 1635, 1540 and 1230 $cm^{-1}$ due to C=O, C=C, NH and P=O stretching, respectively (Figure 4.19). The strong bands in the range of 920–1000 $cm^{-1}$ correspond to the symmetric and asymmetric vibrations of P-O.

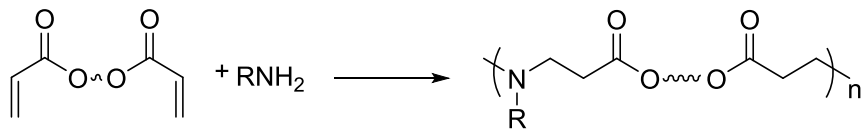


**ACRYLATES**

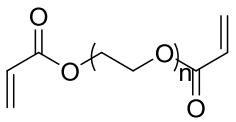

PEGDA

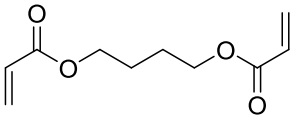

BDDA

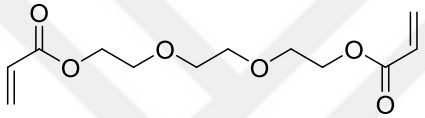

TEGDA

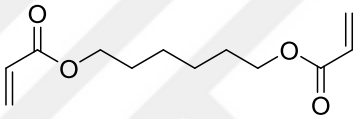

HDDA

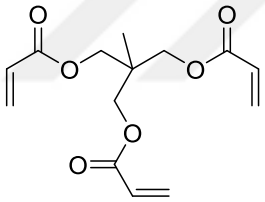

TMPTA

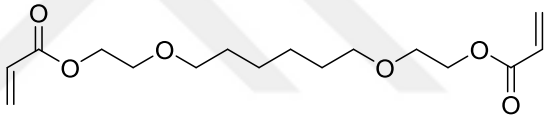

HDEDA

**AMINES**

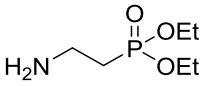


A1

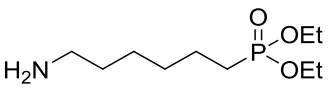


A2

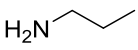


PA

Figure 4.8. Schematic of macromer synthesis, and structures of acrylates and amines

Table 4.1. Solubilities of macromers.

| Macromers | Water | Ether | Petroleum Ether | Choroform | THF | Ethanol | Hexane |
|---|---|---|---|---|---|---|---|
| HDDA-A1 | - | + | - | + | + | + | - |
| HDDA-PA | - | + | - | + | + | + | - |
| BDDA-PA | - | + | - | + | + | + | - |
| BDDA-A1 | - | +/- | - | + | + | + | - |
| HDEDA-PA | - | + | - | + | + | + | - |
| HDEDA-A1 | - | + | - | + | + | + | - |
| PEGDA-PA | + | - | - | + | + | + | - |
| PEGDA-A1 | + | - | + | + | + | + | - |
| PEGDA-TMPTA-A1 | + | - | + | + | + | + | - |
| PEGDA-A2 | +/- | - | - | + | + | + | - |
| TEGDA-A1 | + | - | - | + | + | + | - |

Table 4.2. Repeating units (n) of macromers.

| Macromer (Acrylate : Amine Ratio) | n |
|---|---|
| BDDA-PA (1.2:1) | 3 |
| HDEDA-PA (1.2:1) | 6 |
| PEGDA-A2 (1.2:1) | 2 |
| HDDA-PA (1.2:1) | 4 |
| HDDA-A1 (1.2:1) | 3 |
| HDDA-A1 (1.1:1) | 3-4 |
| BDDA-A1 (1.2:1) | 2 |
| HDEDA-A1 (1.2:1) | 3 |
| TEGDA-A1 (1.2:1) | 2 |
| PEGDA-A1 (1.2:1) | 1-2 |
| PEGDA-PA (1.2:1) | 3 |

Table 4.3. GPC results of some of the macromers.

| **Makromer (Acrylate:Amine ratio)** | **$M_n$** | **PDI** |
|---|---|---|
| HDDA-PA (1.2:1) | 2450 | 1.5 |
| HDDA-A1 (1.2:1) | 1811 | 1.2 |
| HDDA-A1 (1.1:1) | 2745 | 1.4 |
| BDDA-A1 (1.2:1) | 1938 | 1.4 |
| BDDA-PA (1.2:1) | 1842 | 1.4 |
| HDEDA-PA (1.2:1) | 4034 | 1.6 |
| HDEDA-A1 (1.2:1) | 1954 | 1.8 |
| PEGDA-A1 (1.2:1) | 1972 | 1.3 |
| PEGDA-A1 (1.2:1) | 2696 | 1.3 |
| PEGDA-PA (1.2:1) | 3275 | 1.2 |

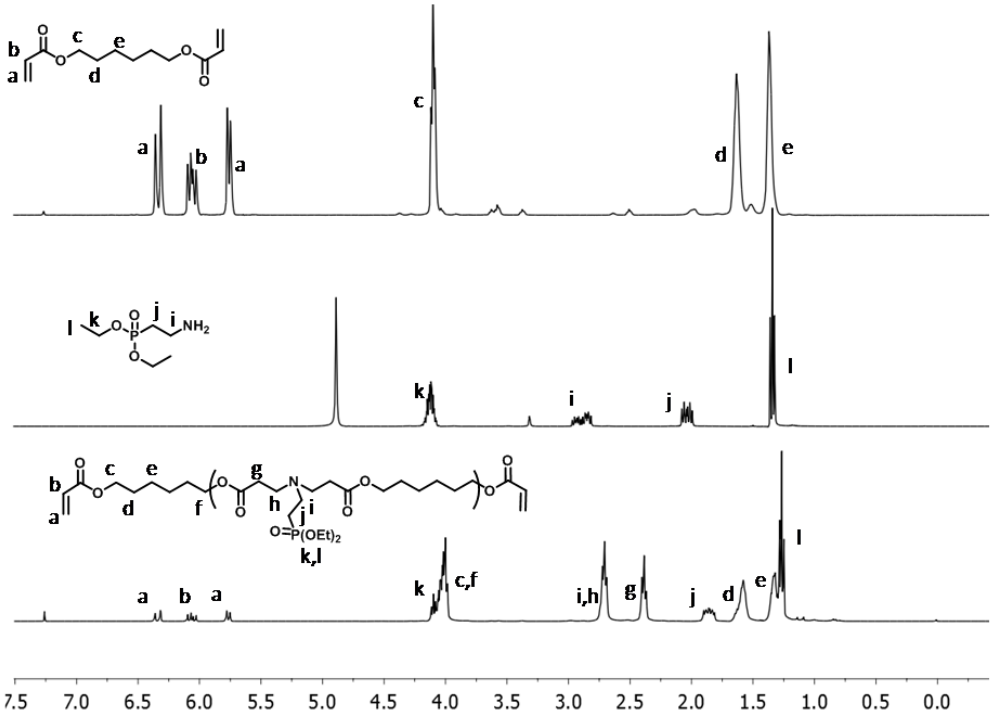


Figure 4.9. [1]H-NMR spectra of HDDA, A1 and HDDA-A1 macromer.

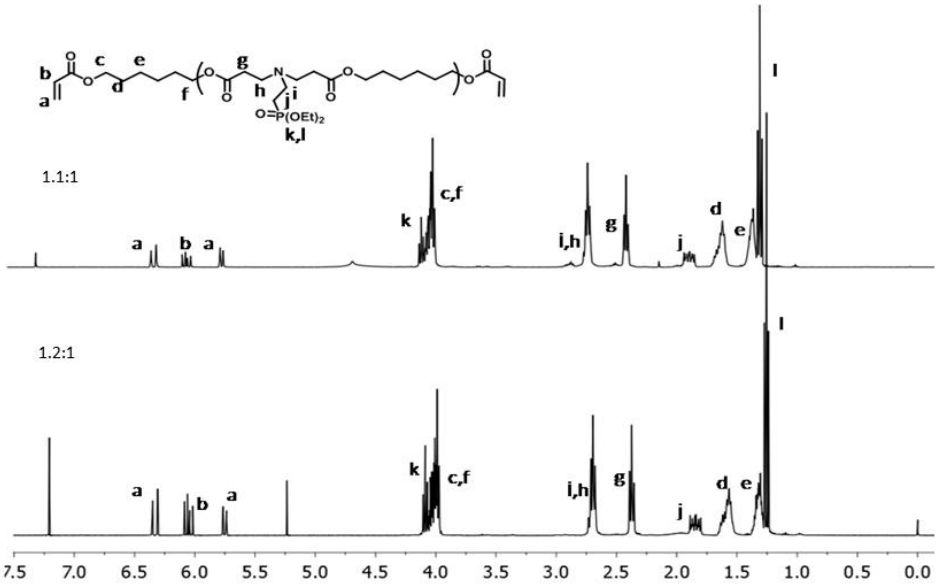


Figure 4.10. $^{1}$H-NMR spectra of HDDA-A1 macromers (diacrylate to amine ratio is 1.1:1 and 1.2:1).

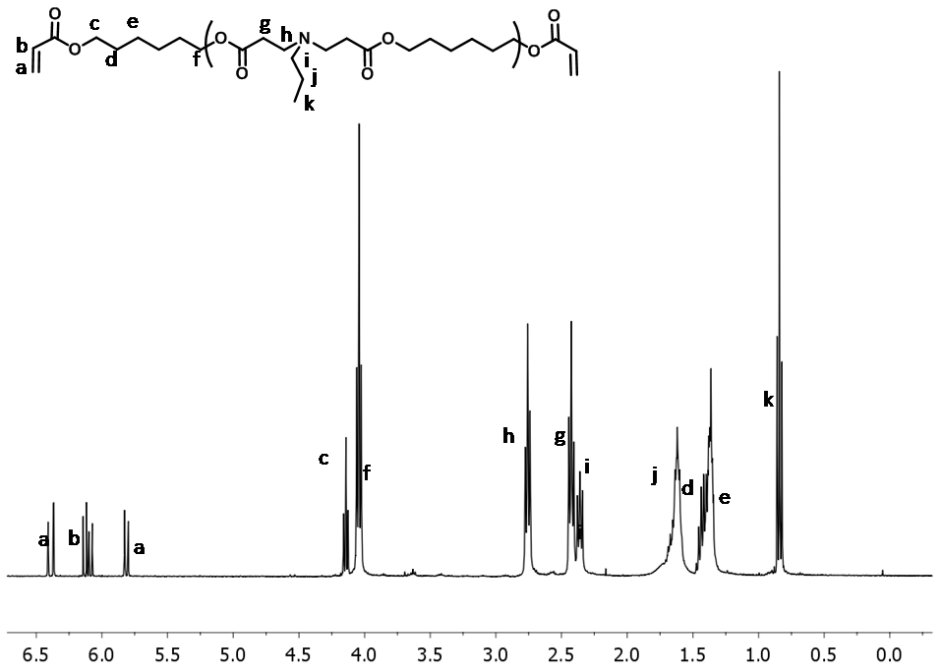


Figure 4.11. $^{1}$H-NMR spectrum of HDDA-PA macromer (diacrylate to amine ratio is 1.2:1).

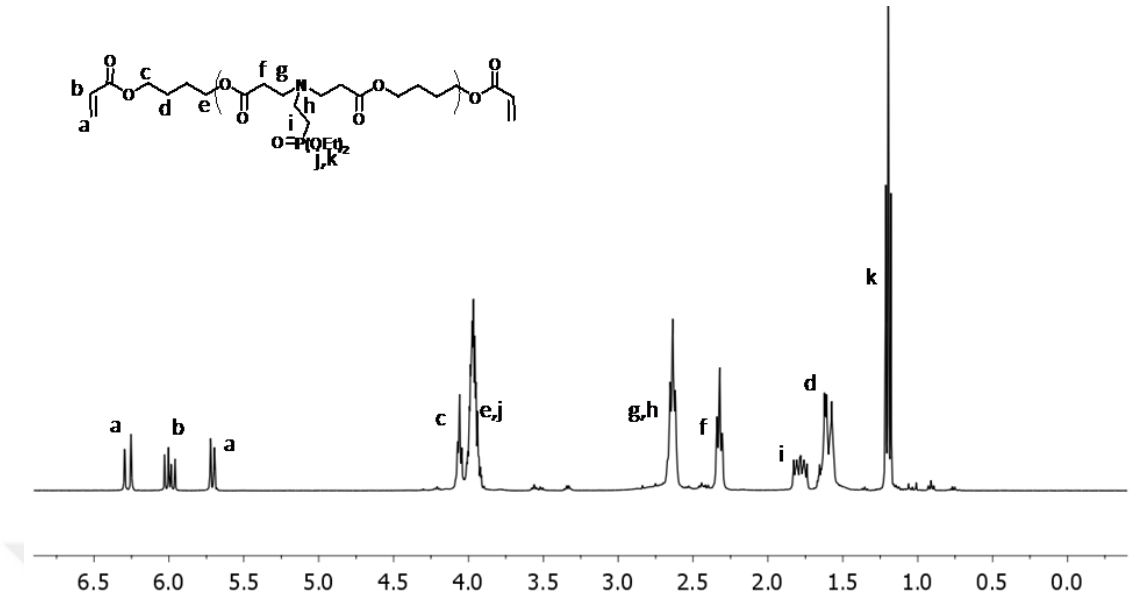


Figure 4.12. $^{1}$H-NMR spectrum of BDDA-A1 macromer (diacrylate to amine ratio is 1.2:1).

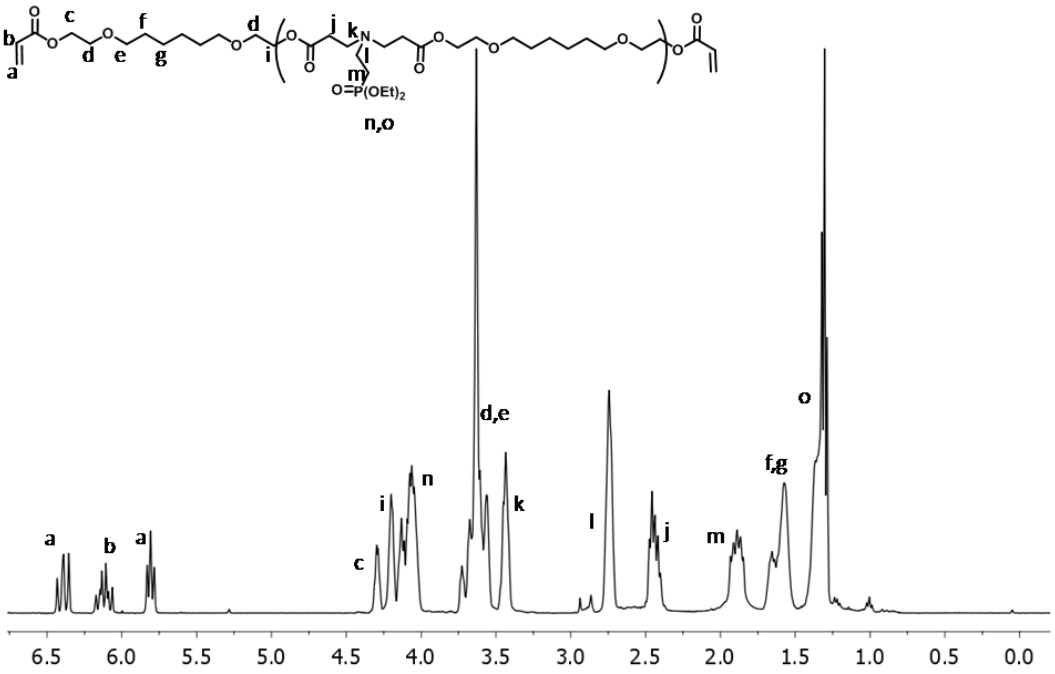


Figure 4.13. $^{1}$H-NMR spectrum of HDEDA-A1 macromer (diacrylate to amine ratio is 1.2:1).

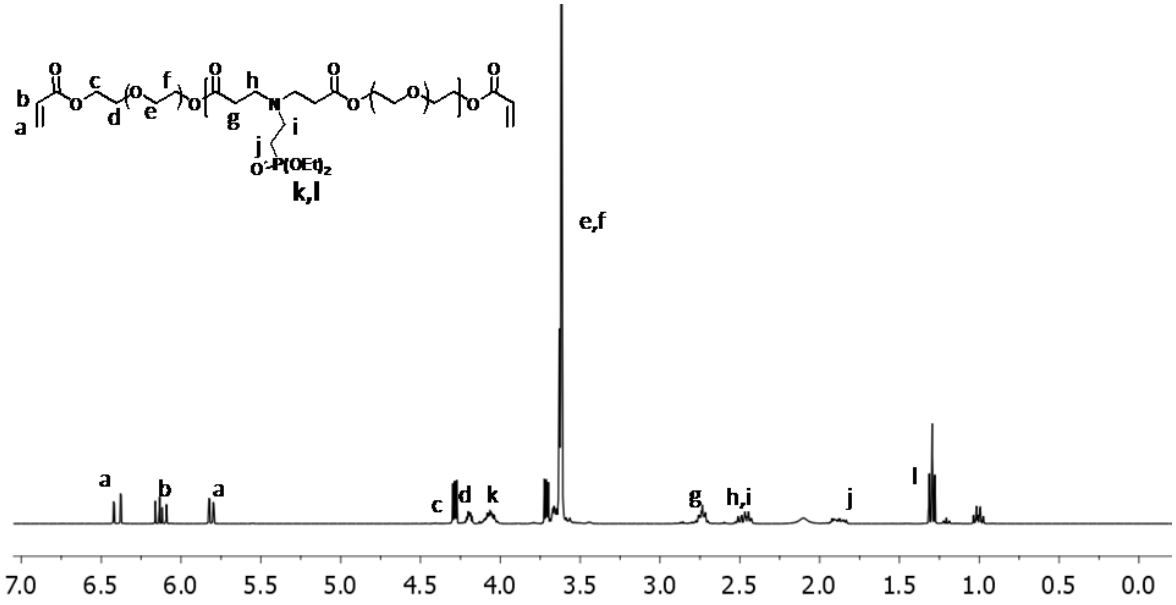


Figure 4.14. $^{1}$H-NMR spectrum of PEGDA-A1 macromer (diacrylate to amine ratio is 1.2:1).

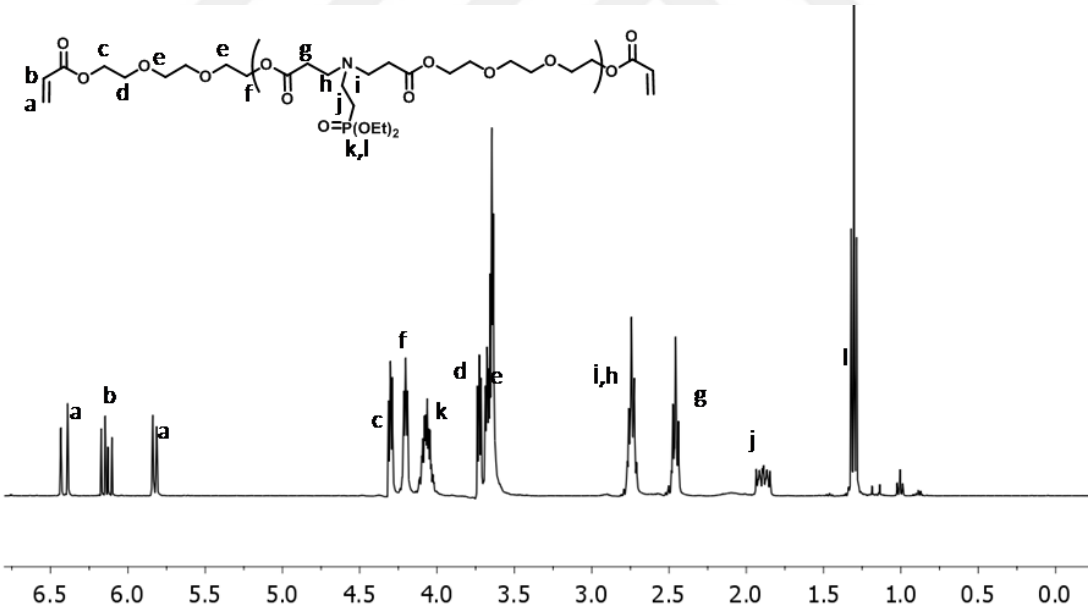


Figure 4.15. $^{1}$H-NMR spectrum of TEGDA-A1 macromer (diacrylate to amine ratio is 1.2:1).

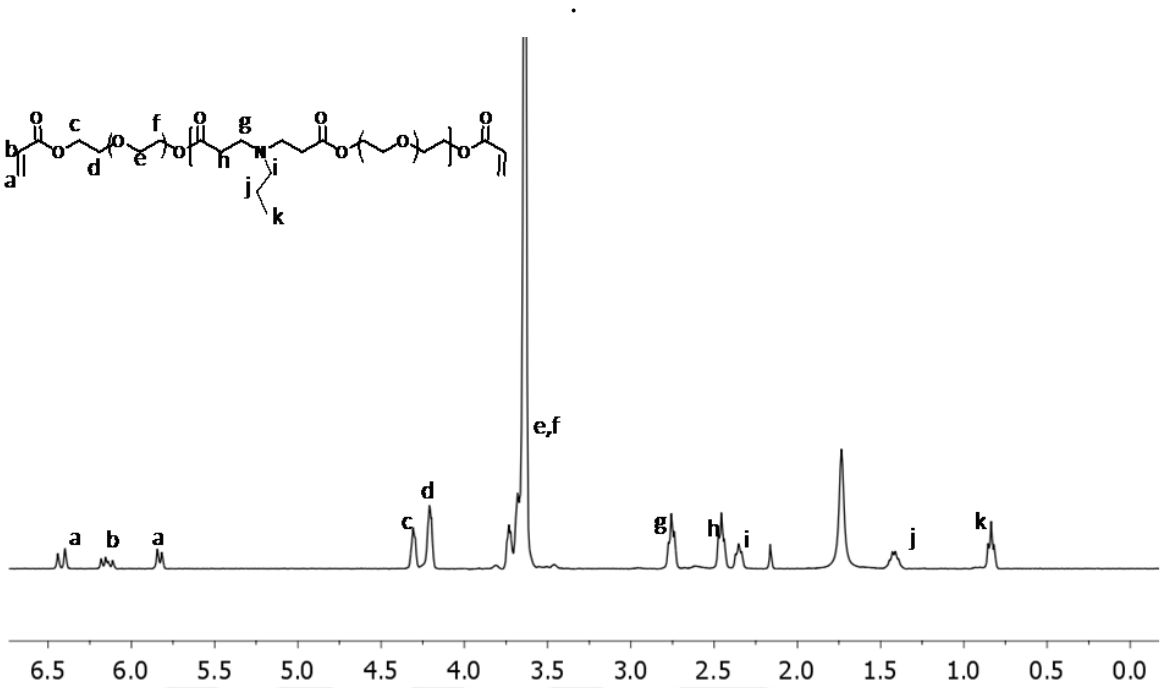


Figure 4.16. [1]H-NMR spectrum of PEGDA-PA macromer (diacrylate to amine ratio is 1.2:1).

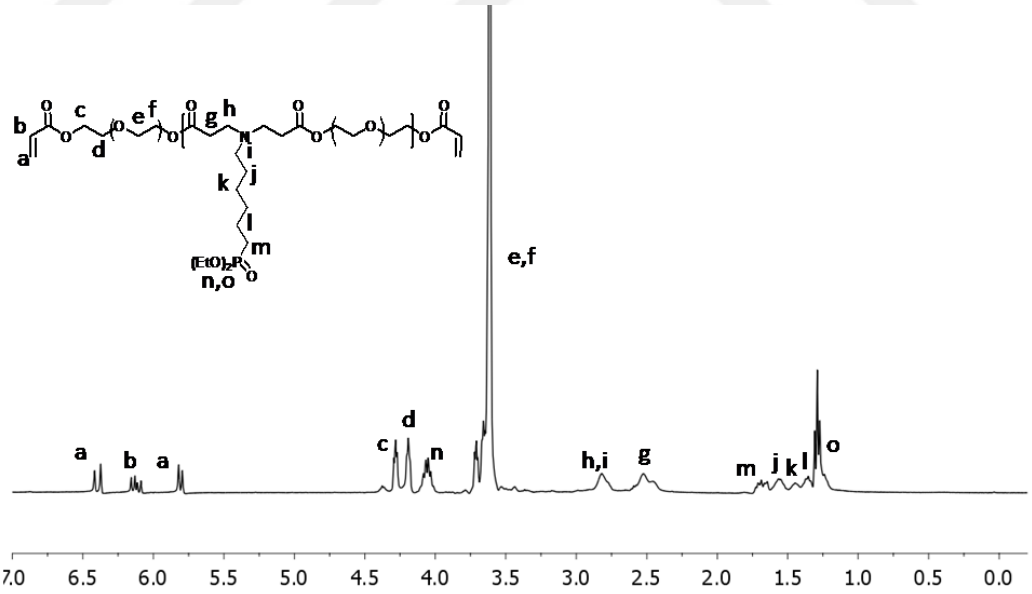


Figure 4.17. [1]H-NMR spectrum of PEGDA-A2 macromer (diacrylate to amine ratio is 1.2:1).

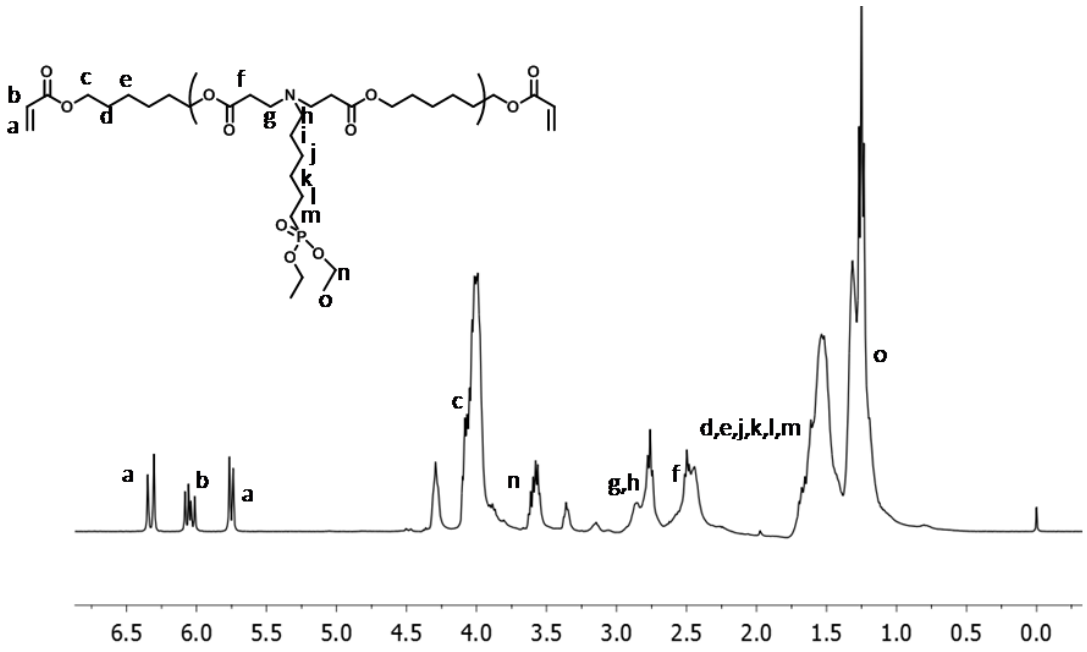


Figure 4.18. $^{1}$H-NMR spectrum of HDDA-A2 macromer (diacrylate to amine ratio is 1.2:1).

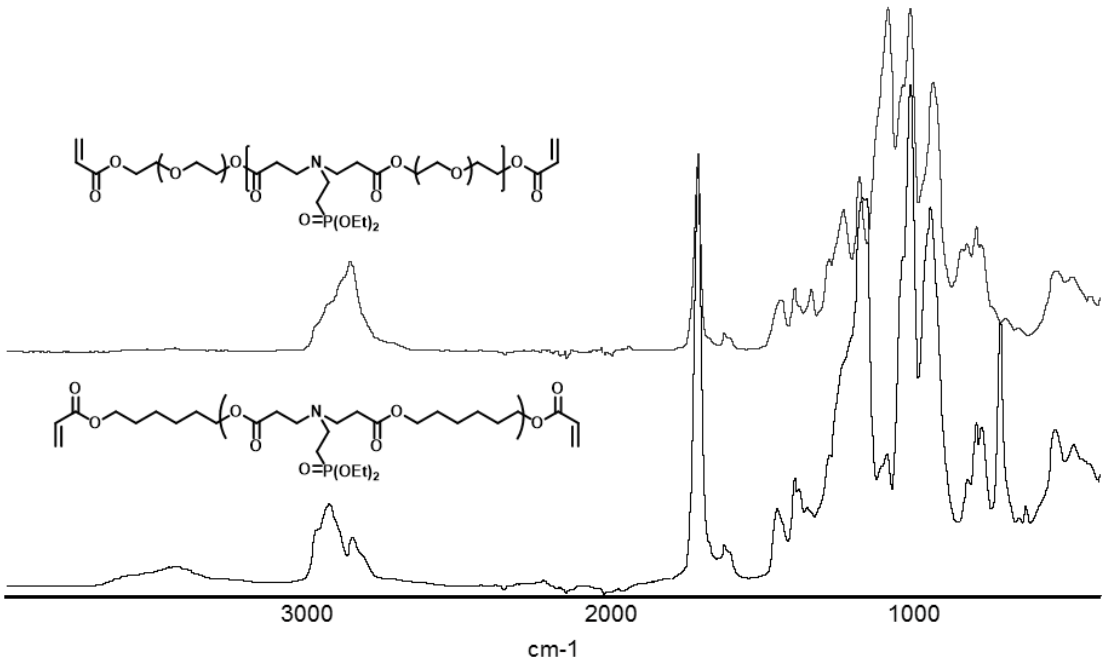


Figure 4.19. FTIR spectra of PEGDA-A1 and HDDA-A1 macromers.

### 4.3. Synthesis of PBAE network polymers

The macromers were bulk photopolymerized into networks using ultraviolet light exposure in the presence of DMPA (1 w %) as photoinitiator at room temperature. The polymerization times ranged from 30 min to 2 h. The soluble fractions due to the lack of complete conversion were removed by placing the samples in ethanol for 24 h. After drying, the percentage of gelation was calculated according to equation (1) and found to range from 46 % to 88%. (Figure 4.20).

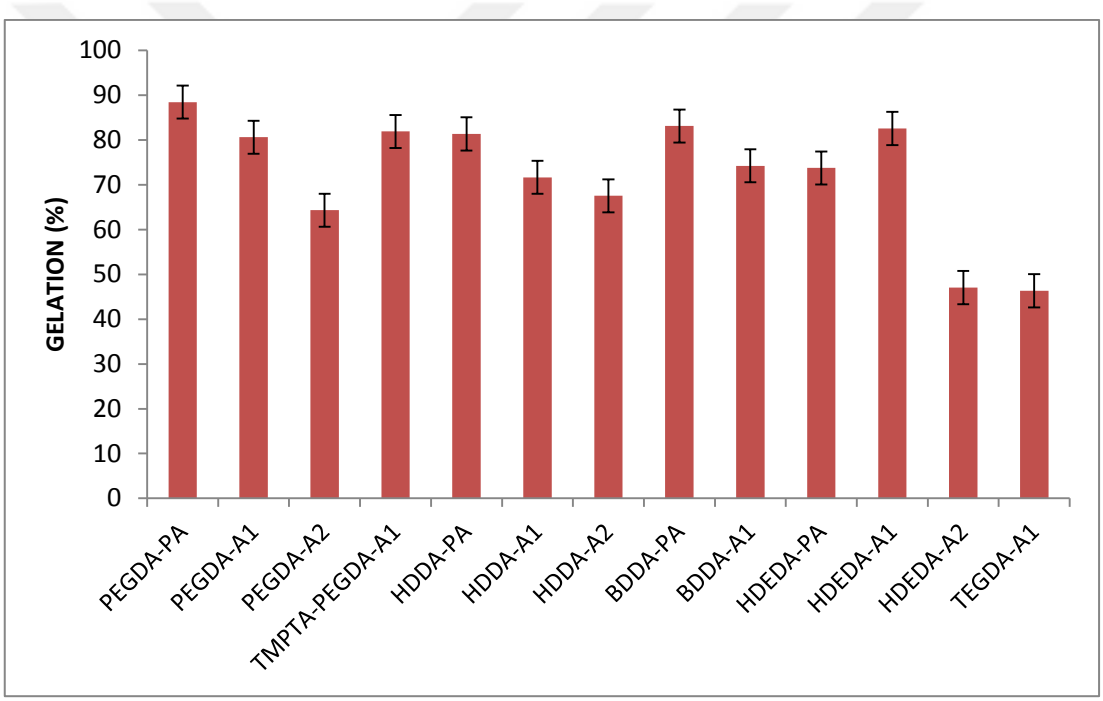


Figure 4.20. Gelation bar of all macromers.

### 4.4. Photopolymerization studies

Photopolymerization reactivities of the synthesized macromers were investigated using real time ATR-FTIR at 25 °C. The decrease in the C=C peak (1635 $cm^{-1}$) with respect to C=O peak (1721 $cm^{-1}$) was monitored during free radical photopolymerization of macromers. The conversion values were calculated from equation (2). Figure 4.21 shows conversion-time plots of some of the macromers.

It was observed that the macromers with a phosphonate group (diacrylate to amine ratio is 1.2:1) in their backbones showed similar conversions ranging from 45 % to 70 % (Figure 4.21). However, polymerization rates observed from the initial slopes of conversion-time plots are different. The highest polymerization rates were observed for HDDA-A1 and HDDA-PA macromers.

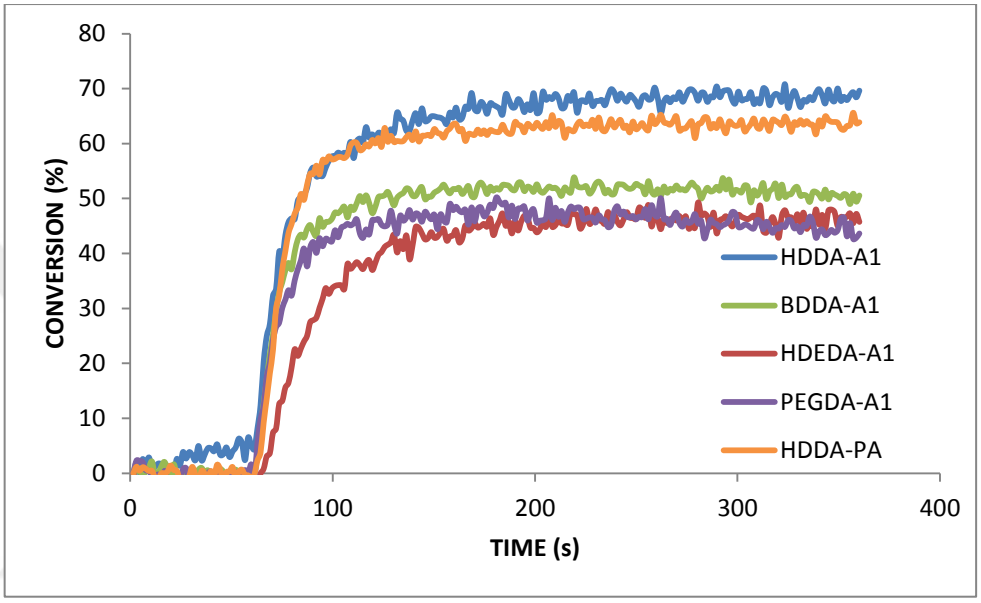


Figure 4.21. Conversion-time plots of some of the macromers.

## 4.5. Degradation Studies

The degradation of the synthesized networks was investigated in PBS at 37 °C after 2, 4 and 8 weeks and the results are shown in Figures 4.22, 4.23. Since the soluble fractions due to unreacted macromers are removed before the tests, there is no rapid mass loss initially. The rate of degradation depends on the structure of the macromers and diacrylate:amine ratios which control the molecular weights. In general, when molecular weight is high, there are more hydrolyzable linkages between the crosslinks which results in higher mass loss.

PEGDA-based polymers (PEGDA-PA and PEGDA-A1) showed higher mass loss than the others, indicating highest degradation rate. The macromer PEGDA-A1's mass loss ranged from 39 to 85 % from 2 weeks to 8 weeks for the 1.2:1 ratio. PEGDA-PA showed

the highest mass loss, which is 97% in 8 weeks. High degradation rate of PEGDA-based monomers are probably due to hydrophilic nature of PEGDA backbone. Addition of the trifunctional monomer TMPTA to the PEGDA and A1 mixture decreased degradation rate as expected. Degradation of the PEGDA-A2 was found to be low due to its hydrophobic structure.

Polymers based on HDDA, BDDA, HDEDA showed similar degradability behavior. Their mass losses were low and around 2-3% after two weeks and increased very slowly up to 18% after 8 weeks. These results indicated that hydrophobic backbone structure is influencing the degradation behavior of the polymers more than the amine substituents.

The degradation of the TEGDA polymers occurs much faster than the HDDA, BDDA and HDEDA polymers but slower than PEGDA-based polymers.

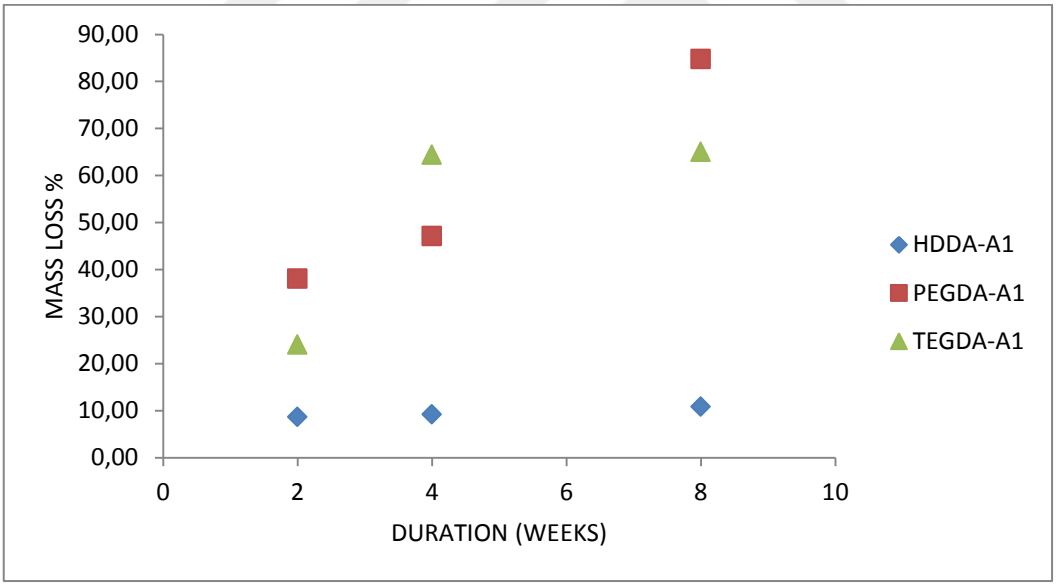


Figure 4.22. Degradation behavior of various polymers.

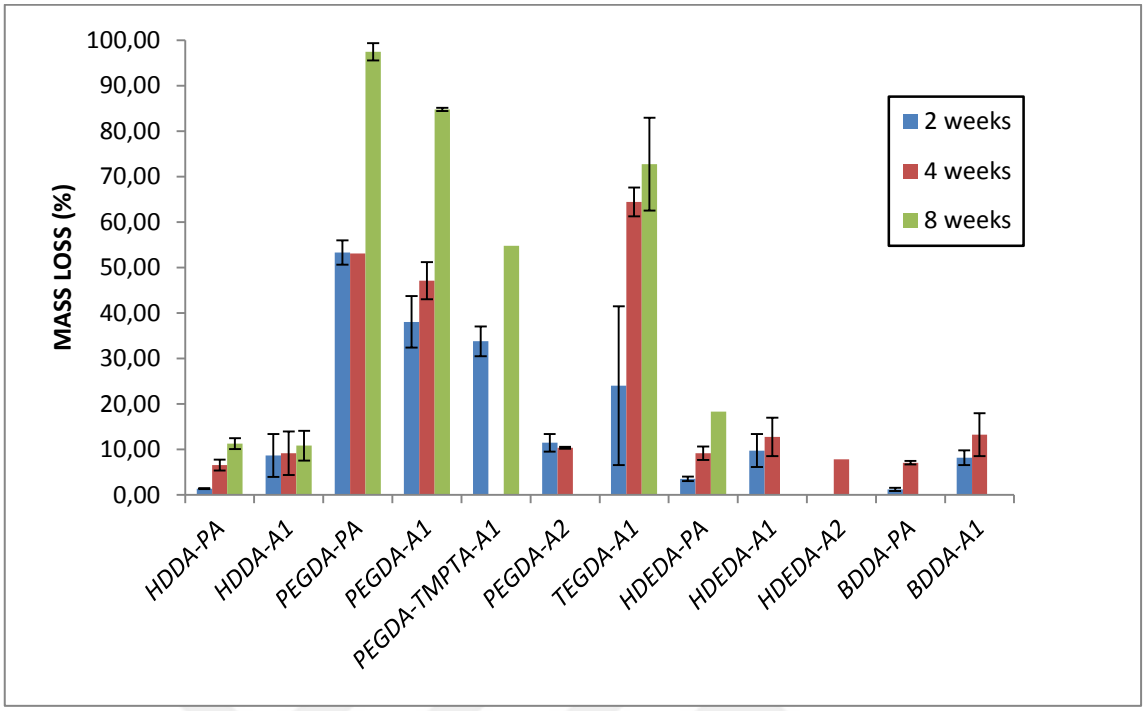


Figure 4.23. Degradation behavior of various polymers after 2, 4 and 8 weeks

## 4.6. In vitro cell interaction

To investigate the effect of polymer structure on cellular interactions, osteoblast-like cells (SaOS-2) were seeded on polymer films formed from the various macromers and cultured for 24h. Films made from PA or A1 with HDDA, BDDA, HDEDA and PEGDA were studied. Films made with these diacrylates and A2, which is a longer chain phosphonated amine, were opaque or colored, hence were not appropriate for the study. For comparison, cells were also cultured on tissue culture polystyrene (TCPS) and also on untreated polystyrene (PS) under the same conditions. All films were prepared on untreated PS plates for two main reasons: 1. Films did not attach well on the TCPS possibly due to the more hydrophobic nature of the macromers; 2. Positive results should represent a true positive, and the possibility of cells attached to TCPS under the polymeric film should be excluded.

Photomicrographs shown in figures 4.24-4.32 represent the attachment, spread, density and the health of cells on these polymeric films. In order to provide a quantitative

comparison of cell attachment on different film surfaces and control plates, the number of attached cells/area were counted (Figure 4.33).

As seen in Figure 4.24 SaOS-2 cells attach nicely and spread on the TCPS plates with nicely elongated structures in 24 h. Yet, although a good number of cells are also found on the untreated PS plate, their attachment and spread is not as good as the those on the TCPS plate. Polystyrene plates are hydrophilically modified for the best attachment and spread of cells as a universal standard.

Figures 4.25 and 4.26 show photomicrographs of cells grown on the surface of the polymers formed from HDDA-PA and HDDA-A1 macromers, respectively. The cells on HDDA-A1 polymers appeared to spread out more than those of HDDA-PA and at least as good as TCPS. No. of attached cells/area also confirms this observation (Figure 4.33). A similar trend was observed with the BDDA-PA (Figure 4.27) and BDDA-A1 (Figure 4.28) polymers. More cells are attached on the latter, although they seem less spread as can be seen from the green stained cytoskeloton. When films made with PA are compared cells attach and spread more on the BDDA-PA films compared to HDDA-PA. In the comparison of HDEDA-PA (Figure 4.29) and HDEDA-A1 (Figure 4.30) polymeric films, it is clearly seen that HDEDA-PA did not allow a significant cell attachment. It was worse than untreated PS and the polymeric films that we have mentioned so far, but HDEDA-A1 stands out as a very good matrix for cell attachment and spread with performance superior to TCPS plate (Figure 4.33).

When PEGDA was used, it was difficult to have a good quality film attached to PS plate surface, both treated and untreated. From the best films, PEGDA-PA did not provide any significant cell attachment (Figure 4.31) and the number of cells and spread was very poor with PEGDA-A1 (Figure 4.32). Possible problems related to the PEGDA films can be (1) the PEG structure itself which is usually used to prevent non-specific cell interaction, (2) fast degradation rate of PEGDA films in PBS compared to others, (3) soft surface due to the most hydrophilic hence most swollen surface.

All these results indicate that chemical structure of the polymeric films has a significant role in cell adhesion. Overall, the presented results indicate that films made with phosphonate containing amines perform better than those made with PA in terms of cell attachment and spread. Films made with A1 (HDDA-A1, HDEDA-A1 and BDDA-A1) were found to support cell attachment almost as good as TCPS or even better. Since all films were made in the untreated-PS and washed well 24h incubation after seeding, we are sure that these cells are attached on the films and are mostly alive. Some cells look round but this may be due to the pre-division stage of cells. Compared to cells that were seeded on TCPS, number of cells/area increases in the following order when used with A1: HDDA>BDDA>HDEDA. This order may represent a decreasing order of hydrophobicity, reaching to an optimum with HDEDA. Structural differences of the diacrylates may also change the surface roughness and stiffness, which do influence the cell attachment. In this case, BDDA may provide a stiffer but more hydrophobic surface than HDDA. Cells are known to attach to rough and stiffer surfaces. Also, as mentioned before, cells attach to hydrophilic surfaces better than hydrophobic ones. Based on the obtained results HDEDA-A1 may bring out a good compromise with a more balanced hydrophilic/hydrophobic nature and an intermediate stiffness.

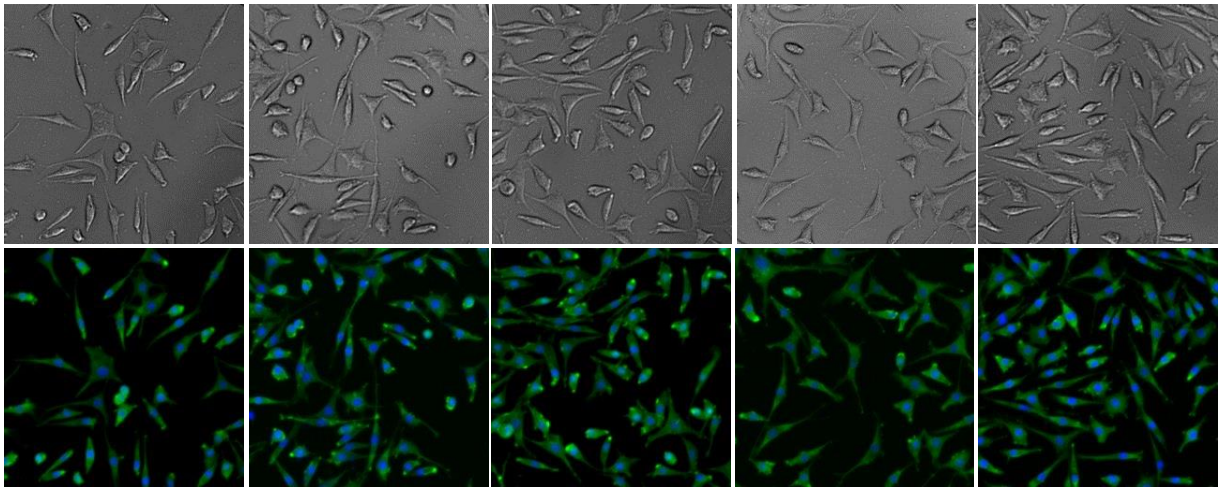

(a)

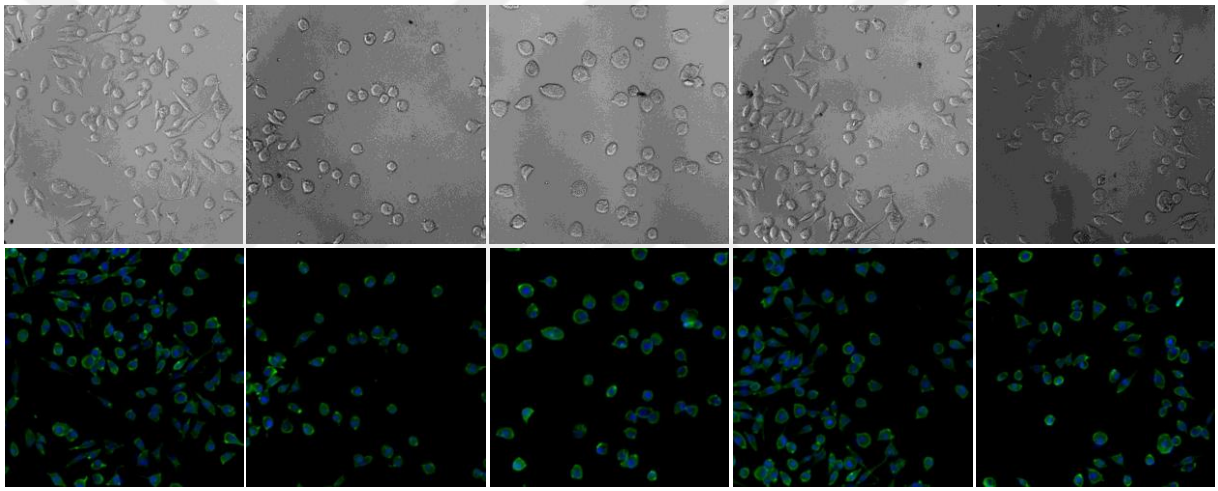

(b)

Figure 4.24. Photomicrographs of SaOS-2 cells 24 h after seeding on (a) TCPS (control, treated polystyrene tissue culture plates), (b) PS (control, untreated polystyrene plates).

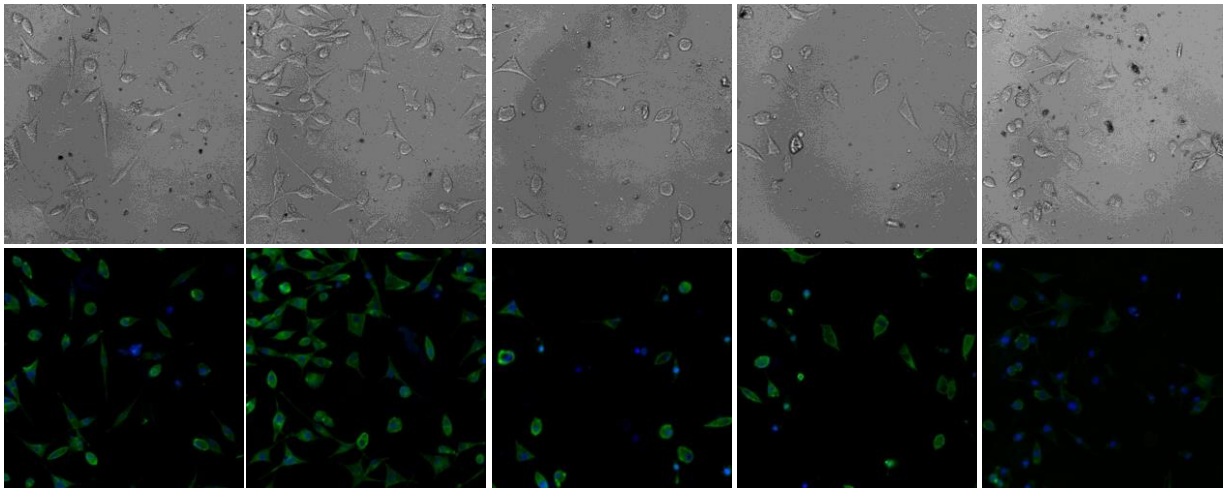

Figure 4.25. Photomicrographs of SaOS-2 cells 24 h after seeding on HDDA-PA polymer.

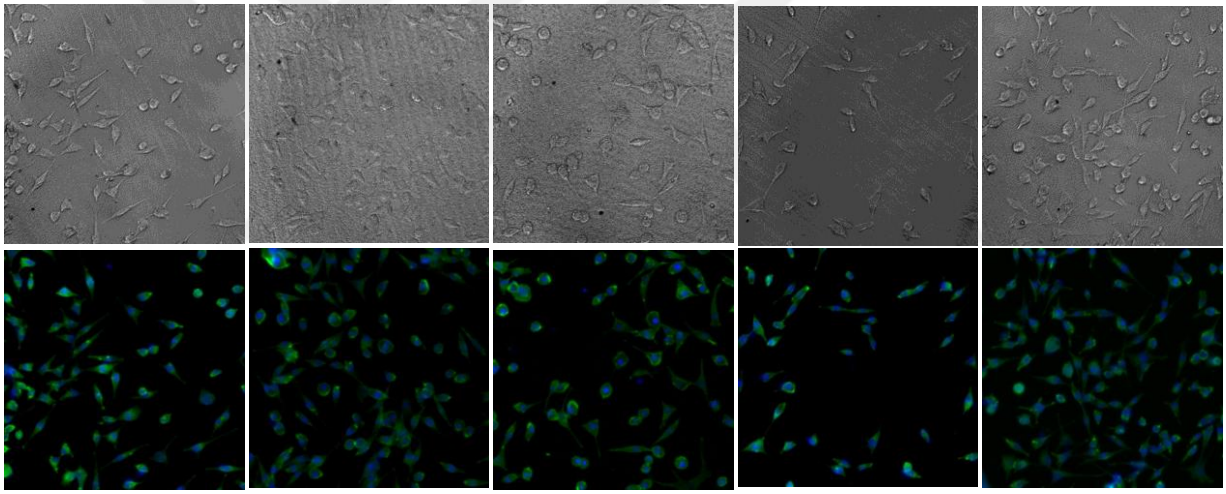

Figure 4.26. Photomicrographs of SaOS-2 cells 24 h after seeding on HDDA-A1 polymer.

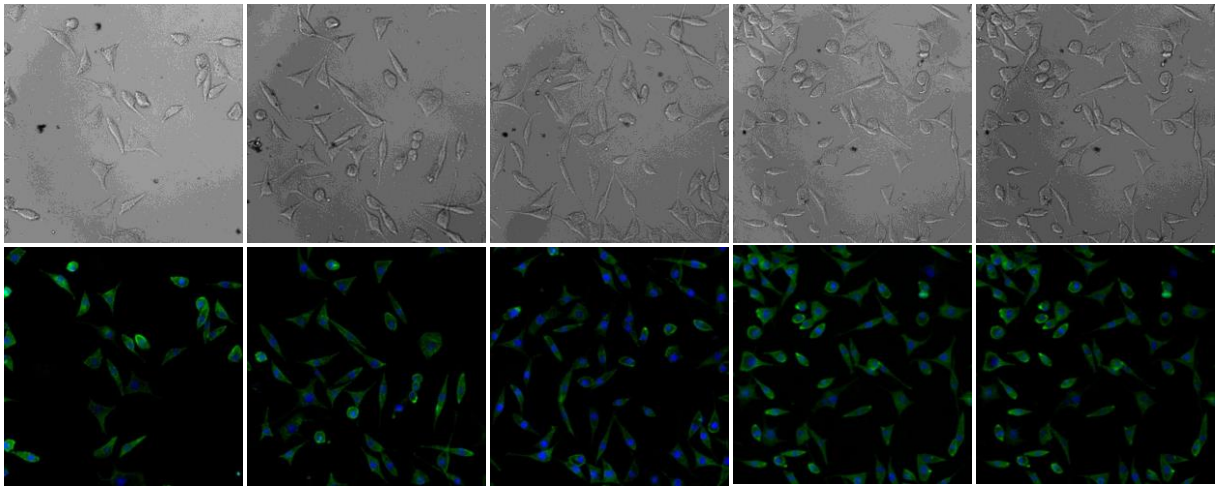

Figure 4.27. Photomicrographs of SaOS-2 cells 24 h after seeding on BDDA-PA polymer.

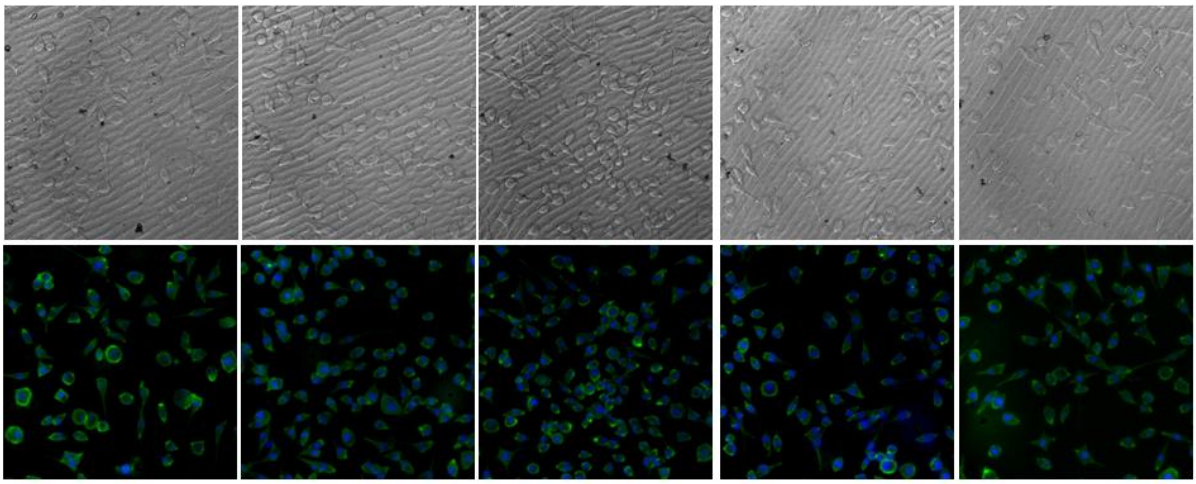

Figure 4.28. Photomicrographs of SaOS-2 cells 24 h after seeding on BDDA-A1 polymer.

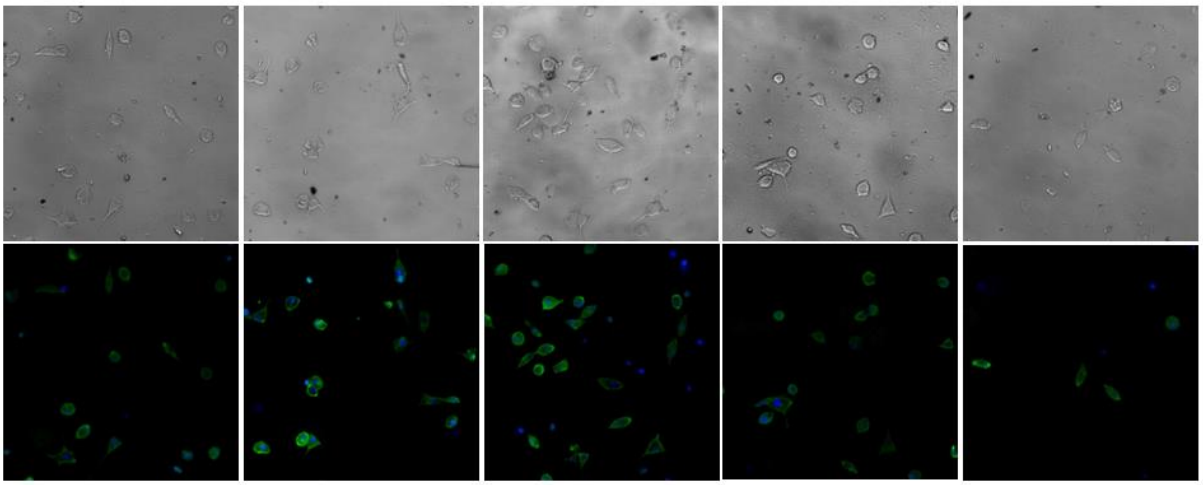

Figure 4.29. Photomicrographs of SaOS-2 cells 24 h after seeding on HDEDA-PA polymer.

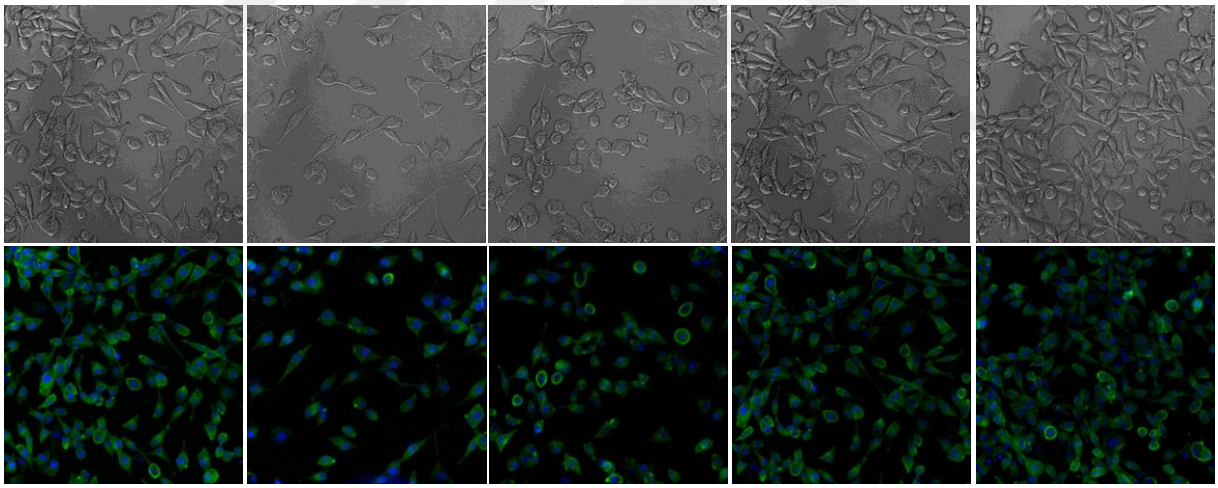

Figure 4.30. Photomicrographs of SaOS-2 cells 24 h after seeding on HDEDA-A1 polymer.

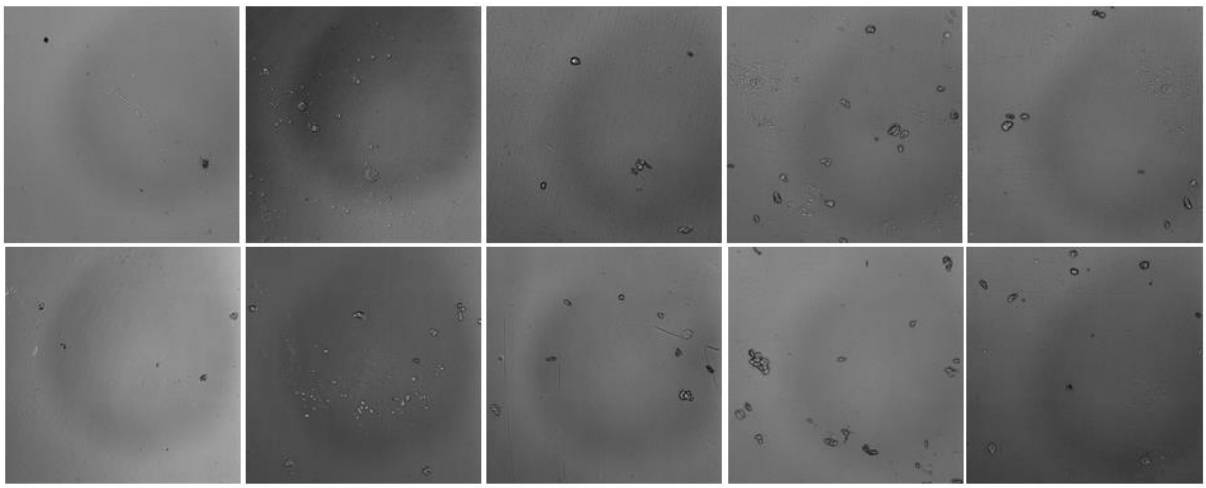

Figure 4.31. Photomicrographs of SaOS-2 cells 24 h after seeding on PEGDA-PA polymer.

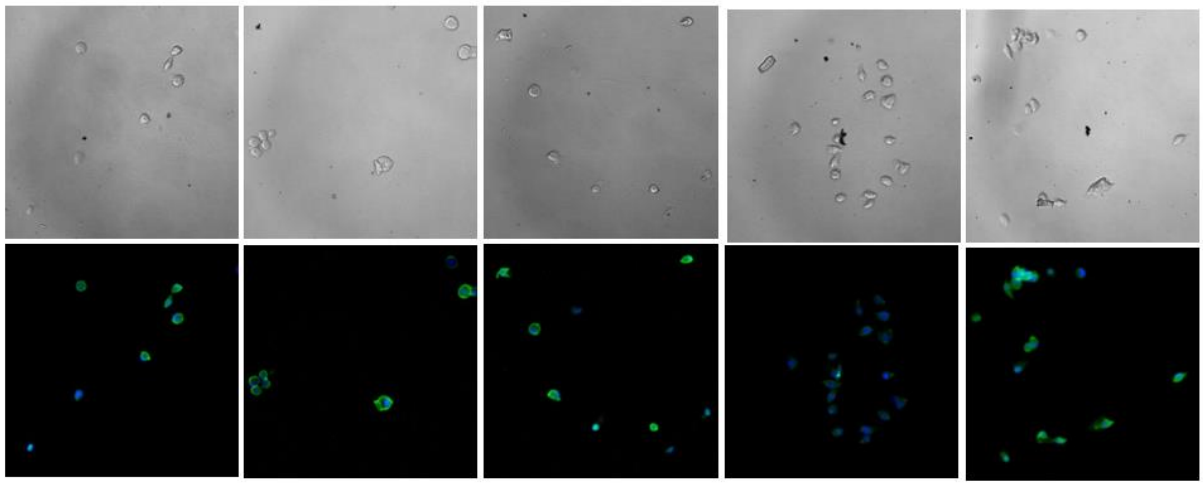

Figure 4.32. Photomicrographs of SaOS-2 cells 24 h after seeding on PEGDA-A1 polymer.

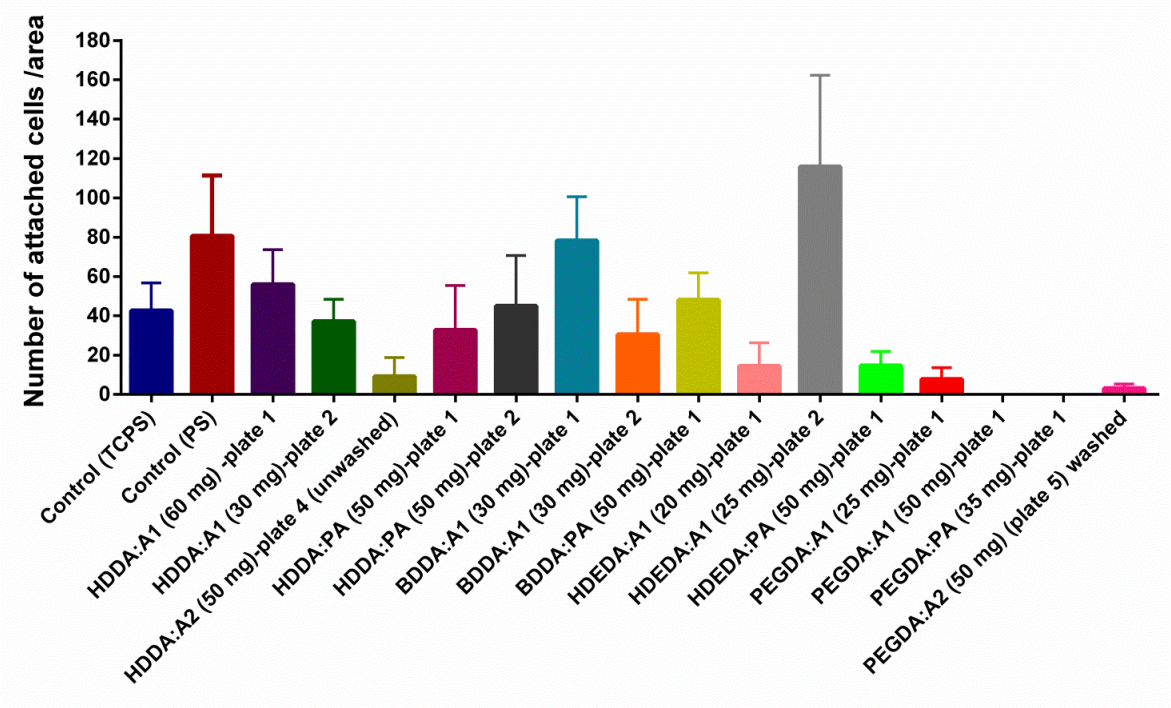


Figure 4.33. Number of attached cells/area for various polymers under different conditions.

## 4.7. In vitro cytotoxicity of polymers

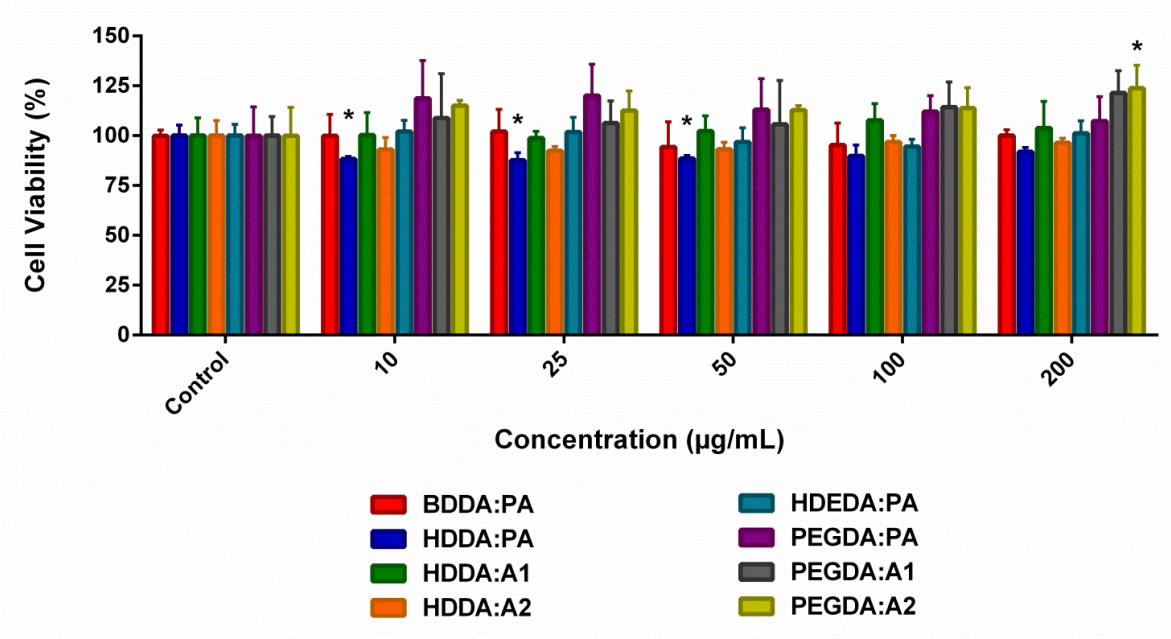


Figure 4.34. Viability of SaOS-2 cells in the presence of degredation products after 24 hours incubation as determined by MTT assay ($p < 0.05$(*), $p < 0.01$ (**), $p < 0.001$ (***) and $p < 0.0001$(****)), (n=4).

The cytotoxicity of the degradation products on SaOS-2 human osteogenic sarcoma cell line was determined by MTT assay (Figure 4.37). In order to determine the relative difference of toxicity between the degradation products, a dose dependent study was performed. Hence, not the amount but the composition of the material incubated with the cells were changed, regardless of the degradation rate. Cell viability above 80 % is assumed as non-cytotoxic, between 80-60 % as weakly, 60–40 % as moderately and below 40 % as strongly cytotoxic according to ISO 10993-5 [44,45]. Based on this there is no significant composition or dose dependent toxicity of the materials tested, except HDDA-PA, which caused a slight toxicity.

# 5. CONCLUSIONS

Novel phosphonate-functionalized PBAE macromers were successfully synthesized and photopolymerized to give network polymers. Their structures were confirmed by $^{1}$H-NMR and FT-IR spectroscopy.

The chemical structure of the polymers (based on the amines and diacrylates chosen for the macromer) affected the degradation properties. The polymers formed from the more hydrophilic macromers (PEGDA-PA, PEGDA-A1) degraded faster than the other polymers (HDDA-A1, BDDA-A1, HDEDA-A1 and TEGDA-A1). Their degradation was found to decrease when a more hydrophobic amine (A2) which contains a six carbon chain was incorporated into the macromer (PEGDA-A2) or by incorporation of a trifunctional acrylates such as TMPTA.

The adhesion and spreading of human SaOS-2 cells on polymer films was also found to be dependent on the chemical structure of the polymers. Although most of the polymers were found to support attachment and spreading of human SaOS-2 cells, one of them (formed from HDEDA-A1 macromer) showed better results. Polymer films formed from three of the phosphorus-containing macromers (HDDA-A1, HDEDA-A1 and BDDA-A1) were found to support cell attachment better than those with no phosphorus (HDDA-PA, HDEDA-PA and BDDA-PA).

The new phosphonated macromers were found to be non-toxic at the tested concentrations.

These results illustrate that incorporation of the phosphonate functional groups into PBAE macromers enables further diversity in photocrosslinkable PBAE properties and that by varying the chemistry and macromer structure, a wide variety of applications can be addressed.

# REFERENCES


1. Tzeng, S.Y., H. Guerrero-Cázares, E.E. Martinez, J.C. Sunshine, A. Quiñones-Hinojosa, and J.J. Green, "Non-viral Gene Delivery Nanoparticles Based On Poly(β-amino Esters) For Treatment Of Glioblastoma.", *Biomaterials*, Vol. 32, pp. 5402–10, 2011.

2. Yin, Q., J. Shen, L. Chen, Z. Zhang, W. Gu, and Y. Li, "Overcoming Multidrug Resistance By Co-delivery Of Mdr-1 and Survivin-targeting RNA With Reduction-responsible Cationic Poly(β-amino Esters).", *Biomaterials*, Vol. 33, pp. 6495–506, 2012.

3. Zhao, J., L. Yang, P. Huang, Z. Wang, Y. Tan, H. Liu, J. Pan, C.-Y. He, and Z.-Y. Chen, "Synthesis And Characterization Of Low Molecular Weight Polyethyleneimine-terminated Poly(β-amino Ester) For Highly Efficient Gene Delivery Of Minicircle DNA.", *Journal of Colloid and Interface Science*, Vol. 463, pp. 93–8, 2016.

4. Zugates, G.T., D.G. Anderson, S.R. Little, I.E.B. Lawhorn, and R. Langer, "Synthesis of Poly(beta-amino Ester)s With Thiol-reactive Side Chains For DNA Delivery.", *Journal of the American Chemical Society*, Vol. 128, pp. 12726–34, 2006.

5. Deng, X., N. Zheng, Z. Song, L. Yin, and J. Cheng, "Trigger-responsive, Fast-degradable Poly(β-amino Ester)s For Enhanced DNA Unpackaging And Reduced Toxicity.", *Biomaterials*, Vol. 35, pp. 5006–15, 2014.

6. Jones, C.H., M. Chen, A. Ravikrishnan, R. Reddinger, G. Zhang, A.P. Hakansson, and B.A. Pfeifer, "Mannosylated Poly(beta-amino Esters) For Targeted Antigen Presenting Cell Immune Modulation.", *Biomaterials*, Vol. 37, pp. 333–44, 2015.

7. Segovia, N., P. Dosta, A. Cascante, V. Ramos, and S. Borrós, "Oligopeptide-terminated Poly(β-amino Ester)s For Highly Efficient Gene Delivery And Intracellular Localization.", *Acta Biomaterialia*, Vol. 10, pp. 2147–58, 2014.

8. Guk, K., H. Lim, B. Kim, M. Hong, G. Khang, and D. Lee, “Acid-cleavable Ketal Containing Poly(β-amino Ester) For Enhanced SiRNA Delivery.”, *International Journal of Pharmaceutics*, Vol. 453, pp. 541–50, 2013.

9. Song, W., Z. Tang, M. Li, S. Lv, H. Yu, L. Ma, X. Zhuang, Y. Huang, and X. Chen, “Tunable PH-sensitive Poly(β-amino Ester)s Synthesized From Primary Amines And Diacrylates For Intracellular Drug Delivery.”, *Macromolecular Bioscience*, Vol. 12, pp. 1375–83, 2012.

10. Shen, Y., H. Tang, Y. Zhan, E.A. Van Kirk, and W.J. Murdoch, “Degradable Poly(β-amino Ester) Nanoparticles For Cancer Cytoplasmic Drug Delivery.”, *Nanomedicine: Nanotechnology, Biology and Medicine*, Vol. 5, pp. 192–201, 2009.

11. Ko, J., K. Park, Y.-S. Kim, M.S. Kim, J.K. Han, K. Kim, R.-W. Park, I.-S. Kim, H.K. Song, D.S. Lee, and I.C. Kwon, “Tumoral Acidic Extracellular PH Targeting Of pH-responsive MPEG-poly(beta-amino Ester) Block Copolymer Micelles For Cancer Therapy.”, *Journal of Controlled Release*, Vol. 123, pp. 109–15, 2007.

12. Tang, S., Q. Yin, Z. Zhang, W. Gu, L. Chen, H. Yu, Y. Huang, X. Chen, M. Xu, and Y. Li, “Co-delivery Of Doxorubicin And RNA Using pH-sensitive Poly (β-amino Ester) Nanoparticles For Reversal Of Multidrug Resistance Of Breast Cancer.”, *Biomaterials*, Vol. 35, pp. 6047–6059, 2014.

13. Meenach, S.A., C.G. Otu, K.W. Anderson, and J.Z. Hilt, “Controlled Synergistic Delivery Of Paclitaxel And Heat From Poly(β-amino Ester)/iron Oxide-based Hydrogel Nanocomposites.”, *International Journal of Pharmaceutics*, Vol. 427, pp. 177–84, 2012.

14. Helaly, F.M., and M.S. Hashem, “Preparation And Characterization Of Poly(β-Amino Ester) Capsules For Slow Release Of Bioactive Material.”, *Journal of Encapsulation and Adsorption Sciences*, Vol. 03, pp. 65–70, 2013.

15. Bui, Q.N., Y. Li, M.-S. Jang, D.P. Huynh, J.H. Lee, and D.S. Lee, "Redox- And PH-Sensitive Polymeric Micelles Based On Poly(β-amino Ester)-Grafted Disulfide Methylene Oxide Poly(ethylene Glycol) For Anticancer Drug Delivery.", *Macromolecules*, Vol. 48, pp. 4046–4054, 2015.

16. Zhang, Y., R. Wang, Y. Hua, R. Baumgartner, and J. Cheng, "Trigger-Responsive Poly(β-amino Ester) Hydrogels.", *ACS Macro Letters*, Vol. 3, pp.693-697, 2014.

17. Anderson, D.G., C.A. Tweedie, N. Hossain, S.M. Navarro, D.M. Brey, K.J. Van Vliet, R. Langer, and J.A. Burdick, "A Combinatorial Library Of Photocrosslinkable And Degradable Materials.", *Advanced Materials*, Vol. 18, pp. 2614–2618, 2006.

18. Brey, D.M., I. Erickson, and J.A. Burdick, "Influence Of Macromer Molecular Weight And Chemistry On Poly(beta-amino Ester) Network Properties And Initial Cell Interactions.", *Journal of Biomedical Materials Research. Part A*, Vol. 85, pp. 731–41, 2008.

19. Brey, D.M., J.L. Ifkovits, R.I. Mozia, J.S. Katz, and J.A. Burdick, "Controlling Poly(β-amino Ester) Network Properties Through Macromer Branching.", *Acta Biomaterialia*, Vol. 4, pp. 207–217, 2008.

20. Tan, A.R., J.L. Ifkovits, B.M. Baker, D.M. Brey, R.L. Mauck, and J.A. Burdick, "Electrospinning Of Photocrosslinked And Degradable Fibrous Scaffolds.", *Journal of Biomedical Materials Research Part A*, Vol. 87A, pp. 1034–1043, 2008.

21. Metter, R.B., J.L. Ifkovits, K. Hou, L. Vincent, B. Hsu, L. Wang, R.L. Mauck, and J.A. Burdick, "Biodegradable Fibrous Scaffolds With Diverse Properties By Electrospinning Candidates From A Combinatorial Macromer Library.", *Acta Biomaterialia*, Vol. 6, pp. 1219–1226, 2010.

22. Biswal, D., P.P. Wattamwar, T.D. Dziubla, and J.Z. Hilt, "A Single-step Polymerization Method For Poly(β-amino Ester) Biodegradable Hydrogels.", *Polymer*, Vol. 52, pp.

5985–5992, 2011.

23. González, G., X. Fernández-Francos, À. Serra, M. Sangermano, X. Ramis, U. Salz, et al., "Environmentally-friendly Processing Of Thermosets By Two-stage Sequential Aza-Michael Addition And Free-radical Polymerization Of Amine–acrylate Mixtures.", *Polymer Chemistry*, Vol. 6, pp. 6987–6997, 2015.

24. McBath, R.A., and D.A. Shipp, "Swelling And Degradation Of Hydrogels Synthesized With Degradable Poly(β-amino Ester) Crosslinkers.", *Polymer Chemistry*, Vol. 1, pp. 860, 2010.

25. Monge, S., B. Canniccioni, A. Graillot, and J.-J. Robin, "Phosphorus-Containing Polymers: A Great Opportunity For The Biomedical Field.", *Biomacromolecules,* Vol. 12, pp. 1973-82, 2011.

26. Moszner, N., and U. Salz, "Recent Developments Of New Components For Dental Adhesives And Composites.", *Macromolecular Materials and Engineering*, Vol. 292, pp. 245–271, 2007.

27. Sahin, G., D. Avci, O. Karahan, and N. Moszner, "Synthesis And Photopolymerizations Of New Phosphonated Methacrylates From Alkyl A-hydroxymethacrylates And Glycidyl Methacrylate.", *Journal of Applied Polymer Science*, Vol. 114, pp. 97–106, 2009.

28. Akgun, B., and D. Avci, "Synthesis And Evaluations Of Bisphosphonate-containing Monomers For Dental Materials.", *Journal of Polymer Science Part A: Polymer Chemistry*, Vol. 50, pp. 4854–4863, 2012.

29. Altin, A., B. Akgun, Z. Sarayli Bilgici, S. Begum Turker, and D. Avci, "Synthesis, Photopolymerization, And Adhesive Properties Of Hydrolytically Stable Phosphonic Acid-containing (Meth)acrylamides.", *Journal of Polymer Science Part A: Polymer Chemistry*, Vol. 52, pp. 511–522, 2014.

30. Wang, D., Miller S., Sima M., Kopečková P., and Kopeček J.*, “Synthesis And Evaluation Of Water-Soluble Polymeric Bone-Targeted Drug Delivery Systems.”, *Bioconjugate Chemistry.*, Vol. 14, pp. 853-859, 2003.

31. Hulsart-Billström, G., P.K. Yuen, R. Marsell, J. Hilborn, S. Larsson, and D. Ossipov, “Bisphosphonate-Linked Hyaluronic Acid Hydrogel Sequesters And Enzymatically Releases Active Bone Morphogenetic Protein-2 For Induction Of Osteogenic Differentiation.”, *Biomacromolecules*, Vol. 14, pp. 3055-63, 2013.

32. Stancu, I.C., R. Filmon, F. Grizon, C. Zaharia, C. Cincu, M.F. Baslé, and D. Chappard, “The In Vivo Calcification Capacity Of A Copolymer, Based On Methacryloyloxyethyl Phosphate, Does Not Favor Osteoconduction.”, *Journal of Biomedical Materials Research. Part A*, Vol. 69, pp. 584–9, 2004.

33. Wang, L., M. Zhang, Z. Yang, B. Xu, B.E. Hillner, C.S. Cho, et al., “The First Pamidronate Containing Polymer And Copolymer.”, *Chemical Communications*, Vol. 21, pp. 2795, 2006.

34. Gemeinhart, R.A., C.M. Bare, R.T. Haasch, and E.J. Gemeinhart, “Osteoblast-like Cell Attachment To And Calcification Of Novel Phosphonate-containing Polymeric Substrates.”, *Journal of Biomedical Materials Research Part A*, Vol. 78A, pp. 433–440, 2006.

35. Wang, D., C.G. Williams, Q. Li, B. Sharma, and J.H. Elisseeff, “Synthesis And Characterization Of A Novel Degradable Phosphate-containing Hydrogel.”, *Biomaterials*, Vol. 24, pp. 3969–3980, 2003.

36. Wang, D.-A., C.G. Williams, F. Yang, N. Cher, H. Lee, and J.H. Elisseeff, “Bioresponsive Phosphoester Hydrogels For Bone Tissue Engineering.”, *Tissue Engineering*, Vol. 11, pp. 201-213, 2005.

37. Yang, X., S. Akhtar, S. Rubino, K. Leifer, J. Hilborn, and D. Ossipov, "Direct ″Click″ Synthesis Of Hybrid Bisphosphonate–Hyaluronic Acid Hydrogel In Aqueous Solution For Biomineralization.", *Chemistry of Materials*, Vol. 24, pp. 1690-1697, 2012.

38. Bakó, P., T. Novák, K. Ludányi, B. Pete, László Tõke, and G. Keglevich, "D-Glucose-based Azacrown Ethers With A Phosphonoalkyl Side Chain: Application As Enantioselective Phase Transfer Catalysts.", *Tetrahedron: Asymmetry*, Vol. 10, pp. 2373–2380, 1999.

39. Shinkai, S., M. Ishihara, K. Ueda, and O. Manabe, "Photoresponsive Crown Ethers. Part 14. Photoregulated Crown–metal Complexation By Competitive Intramolecular Tail(ammonium)-biting.", *J. Chem. Soc., Perkin Trans. 2*, pp. 511–518, 1985.

40. Gali, H., Prabhu, K. R., Karra, S. R., Katti, K. V., "Facile Ring-Opening Reactions Of Phthalimides As A New Strategy To Synthesize Amide-Functionalized Phosphonates, Primary Phosphines, And Bisphosphines.", *Journal of Organic Chemistry*, Vol. 65, pp. 676-680, 2000.

41. Chen, J., S. Huang, M. Liu, R. Zhuo, "Synthesis and Degradation of Poly(β-aminoester) with Pendant Primary Amine.", *Polymer*, Vol 48, pp. 675-681, 2007.

42. Bhise, N.S., R.S. Gray, J.C. Sunshine, S. Htet, A.J. Ewald, and J.J. Green, "The Relationship Between Terminal Functionalization And Molecular Weight Of A Gene Delivery Polymer And Transfection Efficacy In Mammary Epithelial 2-D Cultures And 3-D Organotypic Cultures.", *Biomaterials*, Vol. 31, pp. 8088–96, 2010.

43. Abramoff, M.D., P.J. Magalhães, and S.J. Ram, "Image Processing With ImageJ.", *Biophotonics International*, Vol. 11, pp. 36–42, 2004.

44. López-García, J., M. Lehocký, P. Humpolíček, and P. Sáha, "HaCaT Keratinocytes Response On Antimicrobial Atelocollagen Substrates: Extent Of Cytotoxicity, Cell Viability And Proliferation.", *Journal of Functional Biomaterials*, Vol. 5, pp. 43–57,

2014.

45. I. O. F. Standardization, Geneva, Switzerland, 2009.